NCAM induces CaMKIIα-mediated RPTPα phosphorylation to enhance its catalytic activity and neurite outgrowth

Vsevolod Bodrikov,[1] Vladimir Sytnyk,[1] Iryna Leshchyns'ka,[1] Jeroen den Hertog,[2] and Melitta Schachner[1,3,4]

[1]Zentrum für Molekulare Neurobiologie, Universität Hamburg, 20246 Hamburg, Germany
[2]Hubrecht Laboratory, Netherlands Institute for Developmental Biology, 3584 CT Utrecht, Netherlands
[3]Keck Center for Collaborative Neuroscience and [4]Department of Cell Biology and Neuroscience, Rutgers University, Piscataway, NJ 08854

Receptor protein tyrosine phosphatase α (RPTPα) phosphatase activity is required for intracellular signaling cascades that are activated in motile cells and growing neurites. Little is known, however, about mechanisms that coordinate RPTPα activity with cell behavior. We show that clustering of neural cell adhesion molecule (NCAM) at the cell surface is coupled to an increase in serine phosphorylation and phosphatase activity of RPTPα. NCAM associates with T- and L-type voltage-dependent Ca^{2+} channels, and NCAM clustering at the cell surface results in Ca^{2+} influx via these channels and activation of NCAM-associated calmodulin-dependent protein kinase IIα (CaMKIIα). Clustering of NCAM promotes its redistribution to lipid rafts and the formation of a NCAM–RPTPα–CaMKIIα complex, resulting in serine phosphorylation of RPTPα by CaMKIIα. Overexpression of RPTPα with mutated Ser180 and Ser204 interferes with NCAM-induced neurite outgrowth, which indicates that neurite extension depends on NCAM-induced up-regulation of RPTPα activity. Thus, we reveal a novel function for a cell adhesion molecule in coordination of cell behavior with intracellular phosphatase activity.

Introduction

Cell interactions in the nervous system depend on multiple cues acting sequentially or in parallel. Adhesion molecules initiate recognition of the extracellular matrix and other cells, and, as transmembrane receptors, activate intracellular signaling cascades fundamental to all aspects of cell behavior. This line of communication is important not only during ontogenetic development but also in the adult nervous system during functional changes, such as learning, memory, and regeneration after traumatic injury. The neural cell adhesion molecule (NCAM) has been recognized as an important mediator of cell interactions via its extracellular domain, which consists of immunoglobulin-like and fibronectin type III–homologous structures that act as ligand and receptors in homophilic and heterophilic cell interactions. Two of the major isoforms of NCAM with molecular masses of 180 kD (NCAM180) and 140 kD (NCAM140) are transmembrane glycoproteins that trigger signaling cascades in the cell interior when clustered either by their natural ligands or by antibodies (Schuch et al., 1989; for review see Maness and Schachner, 2007). Signaling cascades triggered by NCAM have been implicated in neurite outgrowth, neuronal survival, and synaptic plasticity (Rutishauser et al., 1988; Lüthi et al., 1994; Bukalo et al., 2004; Walmod et al., 2004).

The most well-described intracellular signaling pathways activated by NCAM to induce neurite outgrowth and neuronal differentiation include activation of PKC with subsequent NCAM-dependent redistribution of the enzyme to cholesterol-enriched plasma membrane microdomains, so-called lipid rafts, where PKC activates GAP43 (Leshchyns'ka et al., 2003; Korshunova et al., 2007). Association of PKC with NCAM depends on the FGF receptor (Leshchyns'ka et al., 2003), which associates with NCAM and is activated in response to NCAM clustering at the cell surface (Niethammer et al., 2002; Kiselyov et al., 2005).

V. Bodrikov, V. Sytnyk, and I. Leshchyns'ka contributed equally to this paper.

Correspondence to Melitta Schachner: melitta.schachner@zmnh.uni-hamburg.de

Abbreviations used in this paper: BisI, bisindolylmaleimide I; CaM, calmodulin; CaMKIIα, CaM-dependent protein kinase IIα; GAPDH, glyceraldehyde-3-phosphate dehydrogenase; GPI, glycosylphosphatidylinositol; NCAM, neural cell adhesion molecule; RPTPα, receptor protein tyrosine phosphatase α; RPTPα-ID, intracellular domains of RPTPα; RPTPαWT, wild-type RPTPα; VDCC, voltage-dependent Ca^{2+} channels.

The online version of this paper contains supplemental material.

The Rockefeller University Press $30.00
J. Cell Biol. Vol. 182 No. 6 1185–1200
www.jcb.org/cgi/doi/10.1083/jcb.200803045

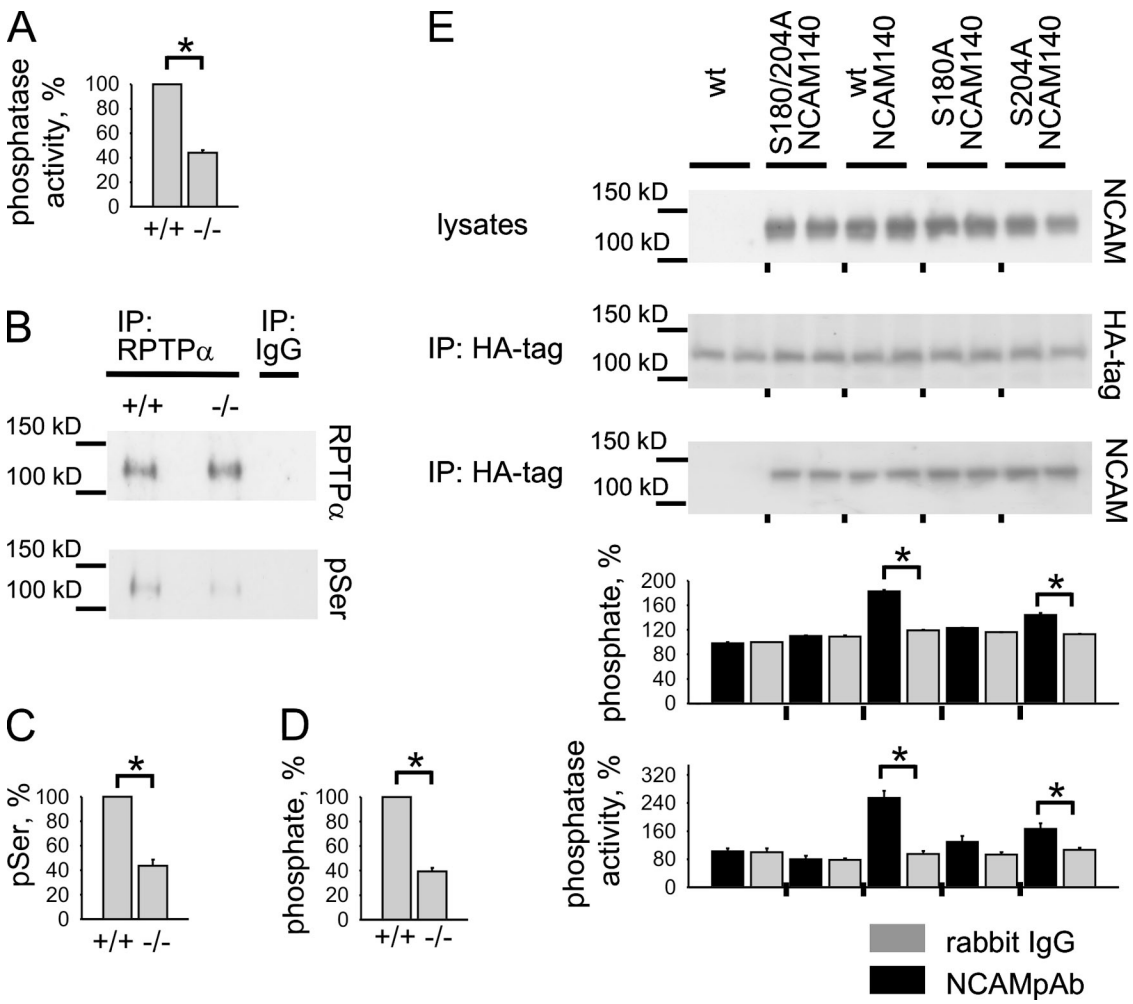

Figure 1. **NCAM140 clustering induces phosphorylation of RPTPα on Ser180 and Ser204 and enhances the phosphatase activity of RPTPα.** (A) Graph shows phosphatase activity of RPTPα from NCAM+/+ and NCAM−/− brain lysates. (B–D) RPTPα immunoprecipitates were probed by Western blotting with antibodies against RPTPα and phospho serines (B and C) or subjected to serine phosphorylation estimation by the alkaline hydrolysis (D). Note that similar levels of RPTPα were immunoprecipitated from NCAM+/+ and NCAM−/− brain lysates (B). Mock immunoprecipitation with nonspecific IgG served as a control. Phosphatase activity and serine phosphorylation of RPTPα are reduced in NCAM−/− brains. Graph in C shows quantitation of the blots in B with optical density for NCAM+/+ brains set to 100%. In A and D, mean values of phosphatase activity (A) or phosphate released by alkaline (D) in RPTPα immunoprecipitates from NCAM+/+ brains were set to 100%. (E) RPTPα-negative fibroblasts transfected with RPTPαWT alone or cotransfected with NCAM140 and RPTPαWT, RPTPαS180A, RPTPαS204A, or RPTPαS180/204A were treated with NCAM polyclonal antibodies or nonspecific rabbit IgG. Note that similar levels of NCAM140 were expressed in cells (lysates) and that similar levels of RPTPα were immunoprecipitated from the lysates (IP: HA-tag). Mutation of Ser180 and/or Ser204 does not influence coimmunoprecipitation of NCAM140 with RPTPα. Immunoprecipitated RPTPα was then subjected to the serine phosphorylation estimation by the alkaline hydrolysis (top) and phosphatase activity analysis (bottom). Application of NCAM antibodies but not IgG increased serine phosphorylation and phosphatase activity of RPTPαWT in NCAM140–RPTPαWT–cotransfected cells. Phosphorylation and activation of RPTPα mutants were inhibited. Mean values of phosphate released by alkaline (top) or phosphatase activity (bottom) in RPTPα immunoprecipitates from IgG-treated NCAM140–RPTPαWT–cotransfected cells were set to 100%. Mean values ± SEM are shown (A and D, $n \geq 8$; C, $n = 6$; E, $n \geq 6$). *, $P < 0.05$ (paired t test).

Another pathway includes activation of p59fyn (hereafter referred to as fyn)/FAK (Beggs et al., 1994, 1997) being induced in response to NCAM clustering or via binding of the glial cell line–derived neurotrophic factor (GDNF) to NCAM (Paratcha et al., 2003). Activation of this pathway depends on NCAM's association with glycosylphosphatidylinositol (GPI)-anchored proteins, such as prion protein (Santuccione et al., 2005) and GFRα1, a cognate receptor for GDNF (Paratcha et al., 2003), and palmitoylation of the intracellular domain of NCAM (Niethammer et al., 2002), linking NCAM to p59fyn enriched in lipid rafts. We have previously found that this pathway is induced by NCAM140, which associates with the receptor protein tyrosine phosphatase α (RPTPα) by direct interaction (Bodrikov et al., 2005). When NCAM is clustered at the neuronal cell surface, the NCAM140–RPTPα complex is further stabilized by the membrane–cytoskeleton linker protein spectrin and redistributes to lipid rafts, where RPTPα binds to and activates fyn (Bodrikov et al., 2005).

We now present evidence that clustering of NCAM at the cell surface results in an enhancement of serine phosphorylation and phosphatase activity of RPTPα. By investigating the mechanisms of NCAM-dependent RPTPα activation, we found that PKCδ, which had been shown in other studies to mediate activation of RPTPα (Brandt et al., 2003), is not involved in NCAM-induced activation. Instead, we identified calmodulin

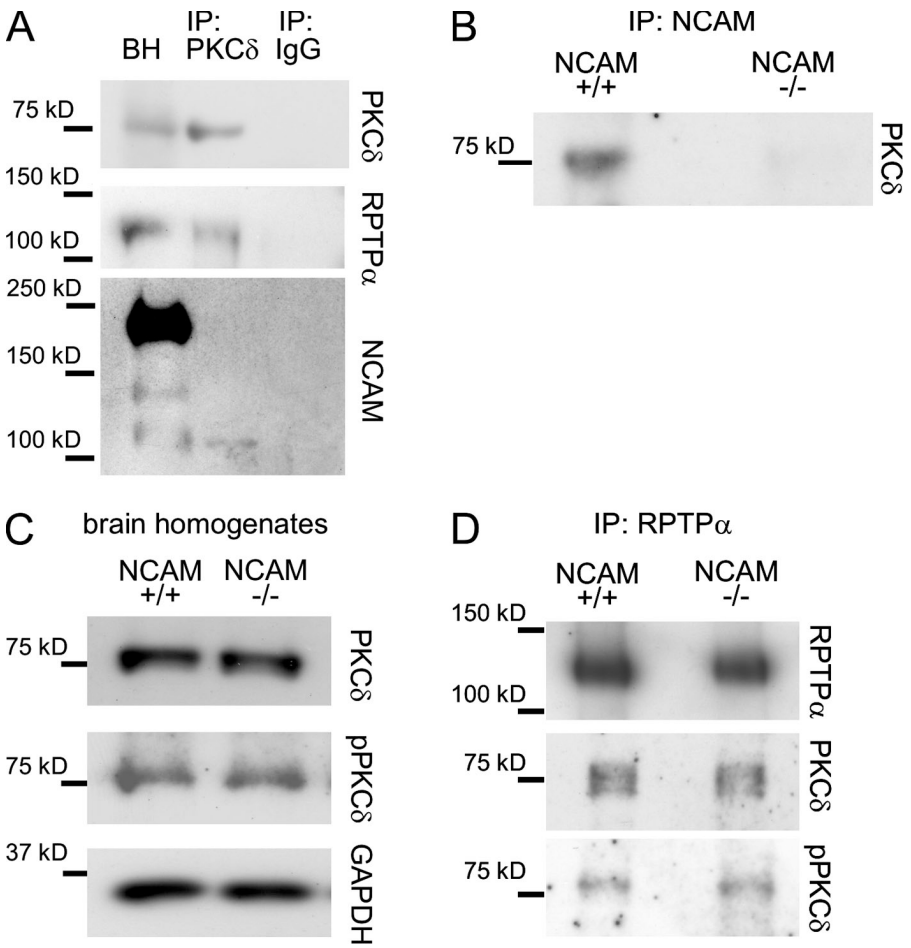

Figure 2. **PKCδ associates with NCAM and RPTPα but its activity is not regulated by NCAM.** (A and B) PKCδ (A) or NCAM (B) immunoprecipitates (IP) from NCAM+/+ brain lysates were analyzed by Western blotting as indicated. Mock immunoprecipitation with nonspecific IgG (A) or from NCAM−/− brain lysates (B) served as a control. RPTPα and NCAM120 coimmunoprecipitate with PKCδ, and PKCδ coimmunoprecipitates with NCAM. BH, brain homogenate. (C and D) NCAM+/+ and NCAM−/− brain homogenates (C) and RPTPα immunoprecipitates from NCAM+/+ and NCAM−/− brain lysates (D) were probed by Western blotting with antibodies against total PKCδ and active Thr505-phosphorylated PKCδ. Note the similar loading (GAPDH labeling in C) and immunoprecipitation efficiency (RPTPα labeling in D). Total levels of active PKCδ and levels of active PKCδ associated with RPTPα are not changed in NCAM−/− brains.

(CaM)-dependent protein kinase IIα (CaMKIIα) as a previously unrecognized enzyme to bind to and phosphorylate RPTPα at two serine residues that increase the phosphatase activity of RPTPα. We show that clustering of NCAM at the cell surface induces lipid raft–dependent activation of CaMKIIα, which then phosphorylates RPTPα at the two serine residues, which, in turn, leads to activation of fyn. Overexpression of RPTPα mutated in both serine residues interferes with NCAM-induced neurite outgrowth of hippocampal neurons in vitro. These observations attribute an important role in the trifunctional interaction between NCAM, CaMKIIα, and RPTPα in lipid rafts and thus add a new dimension in NCAM-mediated signaling pathways.

Results

NCAM up-regulates RPTPα activity by increasing its phosphorylation on Ser180 and Ser204

To analyze the role of NCAM in regulation of the phosphatase activity of RPTPα, RPTPα was immunoprecipitated from NCAM+/+ and NCAM−/− brain lysates. We then used two commercially available phosphotyrosine-containing peptides derived from the epidermal growth factor receptor, which serve as substrates for many protein tyrosine phosphatases, and estimated the efficiency of the release of phosphate from these peptides in the presence of RPTPα immunoprecipitates. This analysis showed that the phosphatase activity of RPTPα from NCAM−/− brains was reduced by ∼55% when compared with RPTPα from NCAM+/+ brains (Fig. 1 A).

Because the phosphatase activity of RPTPα is regulated by phosphorylation, we analyzed phosphorylation of RPTPα by probing RPTPα immunoprecipitates with antibodies against phosphorylated serine residues by Western blotting. In addition, we estimated levels of phosphate released from serine residues of the immunoprecipitated RPTPα by alkaline treatment. Both methods showed that serine phosphorylation of RPTPα was reduced in NCAM−/− brains by ∼60% (Fig. 1, B–D).

Phosphorylation of Ser180 and Ser204 within RPTPα intracellular domain has been shown to be critical for the induction of RPTPα phosphatase activity (Stetak et al., 2001; Zheng et al., 2002). To analyze the role of Ser180 and Ser204 in NCAM-mediated RPTPα regulation, an HA tag containing wild-type RPTPα (RPTPαWT) and RPTPα mutants with Ser180 (RPTPαS180A), Ser204 (RPTPαS204A), or both (RPTPαS180/204A) substituted with alanine were coexpressed with NCAM140 in RPTPα-deficient fibroblasts. Similar levels of NCAM140 coimmunoprecipitated with RPTPαWT and RPTPα mutants from lysates of transfected cells (Fig. 1 E). Thus, mutation of Ser180 and Ser204 does not affect the binding of RPTPα to NCAM. Clustering of NCAM140 at the surface of fibroblasts by NCAM antibodies increased levels of serine phosphorylation of RPTPαWT by ∼200% (Fig. 1 E). In contrast, phosphorylation of RPTPαS180A

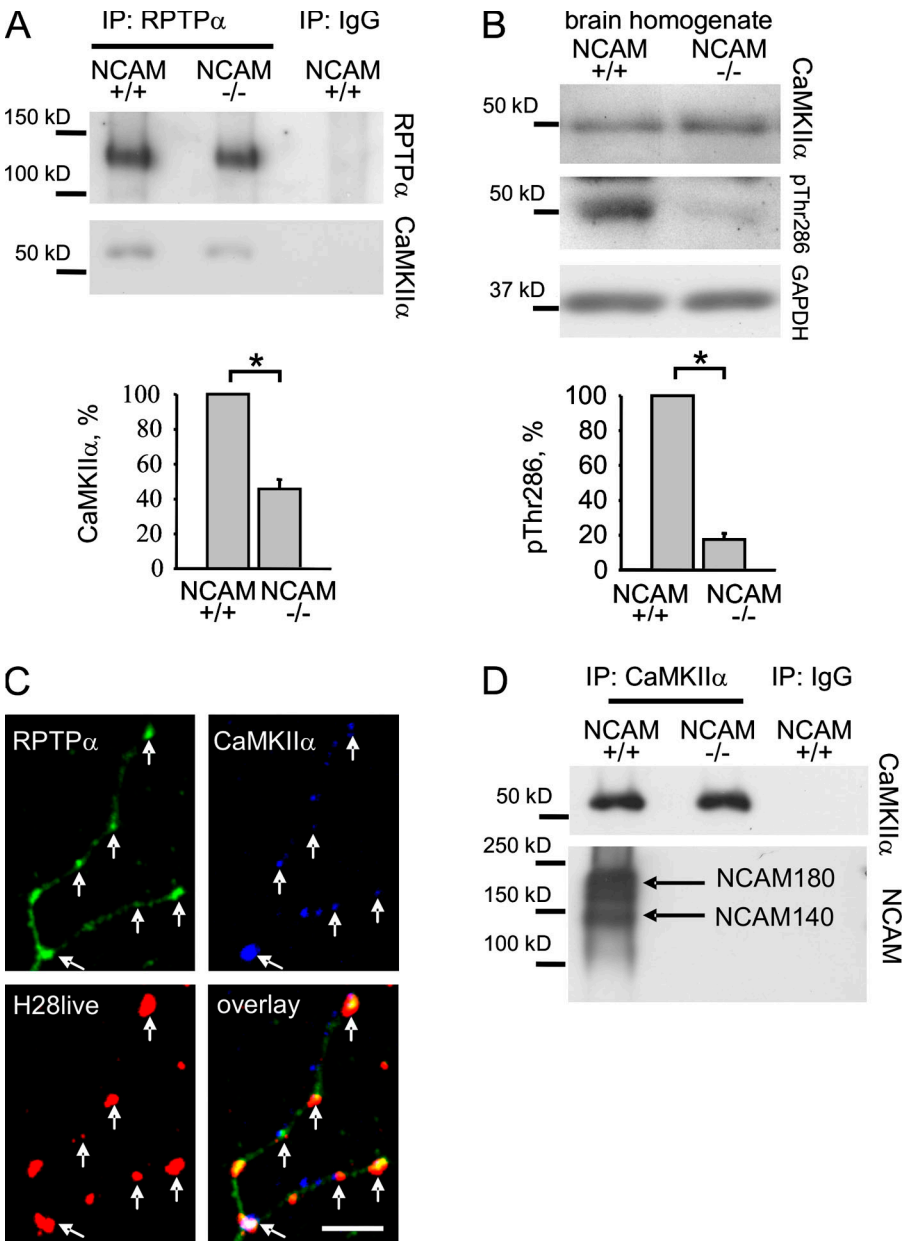

Figure 3. **NCAM promotes CaMKIIα activation and RPTPα–CaMKIIα complex formation.** (A) RPTPα immunoprecipitates (IP) from NCAM+/+ and NCAM−/− brain lysates were probed by Western blotting with antibodies against CaMKIIα. Note that similar levels of RPTPα were immunoprecipitated. Mock immunoprecipitation with nonspecific IgG served as control. Coimmunoprecipitation of CaMKIIα with RPTPα is reduced in NCAM−/− brain lysates. (B) NCAM+/+ and NCAM−/− brain homogenates were probed by Western blotting with antibodies against total and active Thr286-phosphorylated CaMKIIα and GAPDH (loading control). The levels of active CaMKIIα were reduced in NCAM−/− brain homogenates. Graphs show quantitation of the blots (mean ± SEM, $n = 6$ for A and B) with optical density for NCAM+/+ probes set to 100%. *, $P < 0.05$, paired t test. (C) NCAM was clustered at the cell surface of cultured hippocampal neurons by NCAM antibodies (H28live). Neurons were then fixed and colabeled with antibodies against RPTPα and CaMKIIα. A high-magnification image of a neurite is shown. NCAM clusters overlap with accumulations of RPTPα and CaMKIIα (arrows). Bar, 5 µm. (D) CaMKIIα immunoprecipitates from NCAM+/+ and NCAM−/− brain lysates were probed by Western blotting with antibodies against NCAM. NCAM140 and NCAM180 coimmunoprecipitated with CaMKIIα. Mock immunoprecipitation with nonspecific IgG served as a control.

and RPTPαS180/204A in response to NCAM140 clustering was blocked, whereas phosphorylation of RPTPαS204A was partially inhibited (Fig. 1 E). Hence, Ser180 and Ser204 are phosphorylated in response to NCAM140 clustering, with Ser180 being required for NCAM-dependent RPTPα phosphorylation.

Phosphatase activity of RPTPαWT was increased after NCAM140 clustering by ∼250% (Fig. 1 E). Phosphatase activity of RPTPα mutants, however, was reduced when compared with RPTPαWT. Mutation of Ser180 induced a stronger inhibitory effect on the catalytic activity of RPTPα when compared with Ser204 (Fig. 1 E). The catalytic activity of RPTPα was fully inhibited when both Ser180 and Ser204 were mutated (Fig. 1 E). In contrast to fibroblasts transfected with NCAM140, application of NCAM antibodies to the fibroblasts cotransfected with RPTPαWT and NCAM180 or NCAM120 did not result in phosphorylation and activation of RPTPαWT (Fig. S1, available at http://www.jcb.org/cgi/content/full/jcb.200803045/DC1). Hence, NCAM140 is the major NCAM isoform involved in regulation of RPTPα activity.

NCAM does not regulate PKCδ activity and its association with RPTPα

Previous studies indicated that among all PKC isoforms, only PKCδ phosphorylates RPTPα on Ser180 and Ser204 in nonneuronal cells (den Hertog et al., 1995; Tracy et al., 1995; Zheng et al., 2002; Brandt et al., 2003). NCAM associates with and induces activation of several PKC isoforms (Leshchyns'ka et al., 2003; Kolkova et al., 2005), but its role in PKCδ activation has not been analyzed. We thus analyzed whether NCAM regulates RPTPα phosphorylation by inducing PKCδ activation. RPTPα coimmunoprecipitated with PKCδ (Fig. 2 A), and PKCδ coimmunoprecipitated with NCAM (Fig. 2 B) from brain lysates. However, levels of activated PKCδ phosphorylated at Thr505 in the activation loop of the kinase were not changed in NCAM−/− brain homogenates

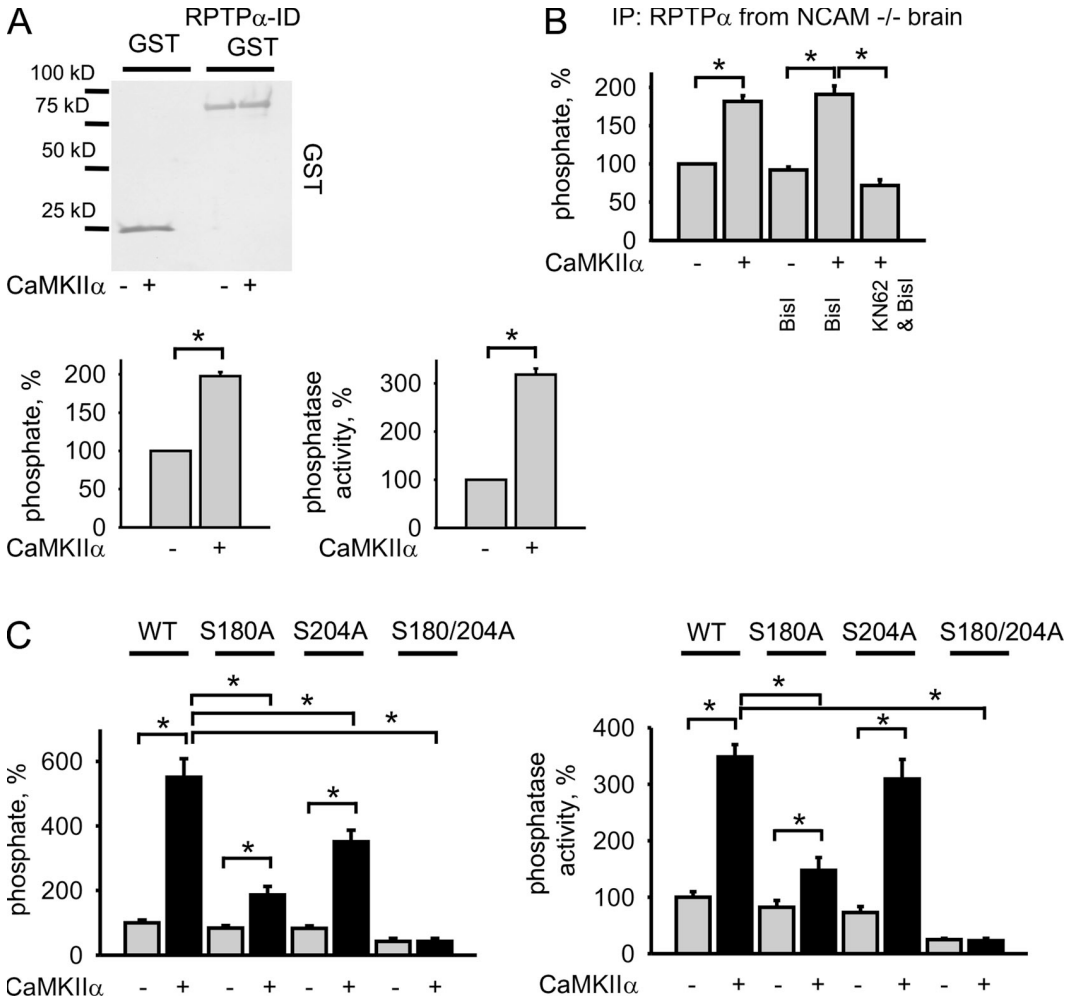

Figure 4. **RPTPα is phosphorylated by CaMKIIα on Ser180 and Ser204.** (A) Recombinant RPTPα-ID-GST or GST coupled to beads were incubated with CaMKIIα. The gel stained with Coomassie blue shows that approximately equal amounts of RPTPα-ID-GST and GST were bound to beads. The beads, treated and nontreated with CaMKIIα, were then subjected to the analysis of serine phosphorylation by alkaline hydrolysis (bottom left) or phosphatase activity (bottom right). Values for GST were subtracted as background, and values of serine phosphorylation (bottom left) or phosphatase activity (bottom right) for RPTPα-ID-GST not treated with CaMKIIα were set to 100%. (B) RPTPα from NCAM−/− brain lysates was incubated with CaMKIIα in the presence or absence of KN62 and Bis1. RPTPα was then subjected to the analysis of serine phosphorylation by alkaline hydrolysis. Values of phosphate released by alkaline from RPTPα not treated with CaMKIIα were set to 100%. (C) RPTPα immunoprecipitated from lysates of RPTPα-negative fibroblasts transfected with RPTPαWT, RPTPαS180A, RPTPαS204A, or RPTPαS180/204A was incubated with CaMKIIα. The immunoprecipitates, treated and untreated with CaMKIIα, were then subjected to the analysis of serine phosphorylation by alkaline hydrolysis (left) or phosphatase activity (right). Mean values of serine phosphorylation (left) or phosphatase activity (right) of RPTPαWT not treated with CaMKIIα were set to 100%. Mean values ± SEM are shown (A, $n = 6$; B, $n = 11$; C, $n = 9$). *, $P < 0.05$ (paired t test).

(Fig. 2 C). Furthermore, similar levels of activated PKCδ coimmunoprecipitated with RPTPα from NCAM+/+ and NCAM−/− brain lysates (Fig. 2 D). Thus, NCAM does not regulate association of RPTPα with PKCδ, nor does it regulate PKCδ activation in the brain. In agreement, the most prominent NCAM isoform that coimmunoprecipitated with PKCδ was the smallest GPI-linked NCAM isoform with a molecular mass of 120 kD (NCAM120; Fig. 2 A). NCAM120 lacks the intracellular domain and therefore probably associates indirectly with PKCδ, as has been shown for spectrin, another intracellular binding partner of NCAM120 that associates with NCAM120 via lipids (Leshchyns'ka et al., 2003).

NCAM induces RPTPα phosphorylation by activating CaMKIIα

CaMKIIα is another serine/threonine protein kinase that associates with NCAM (Sytnyk et al., 2006). CaMKIIα coimmunoprecipitated with RPTPα from brain lysates (Fig. 3 A). Interestingly, binding of CaMKIIα to RPTPα was reduced in NCAM−/− brains (Fig. 3 A). Levels of activated Thr286-phosphorylated CaMKIIα were also reduced in NCAM−/− brains (Fig. 3 B). Hence, NCAM regulates CaMKIIα activation and RPTPα–CaMKIIα complex formation.

In agreement, in cultured hippocampal neurons maintained in vitro for 24 h, CaMKIIα accumulated in growth cones of the growing neurites, where distributions of CaMKIIα and NCAM partially overlapped (see Fig. 7 B). Clustering of NCAM at the cell surface of neurites with NCAM antibodies applied to live neurons induced partial redistribution of RPTPα to NCAM clusters (Fig. 3 C; Bodrikov et al., 2005). Overlapping accumulations of NCAM and RPTPα also colocalized with CaMKIIα aggregates (Fig. 3 C). Thus, CaMKIIα is a likely candidate involved in NCAM140-induced RPTPα phosphorylation accompanying NCAM clustering.

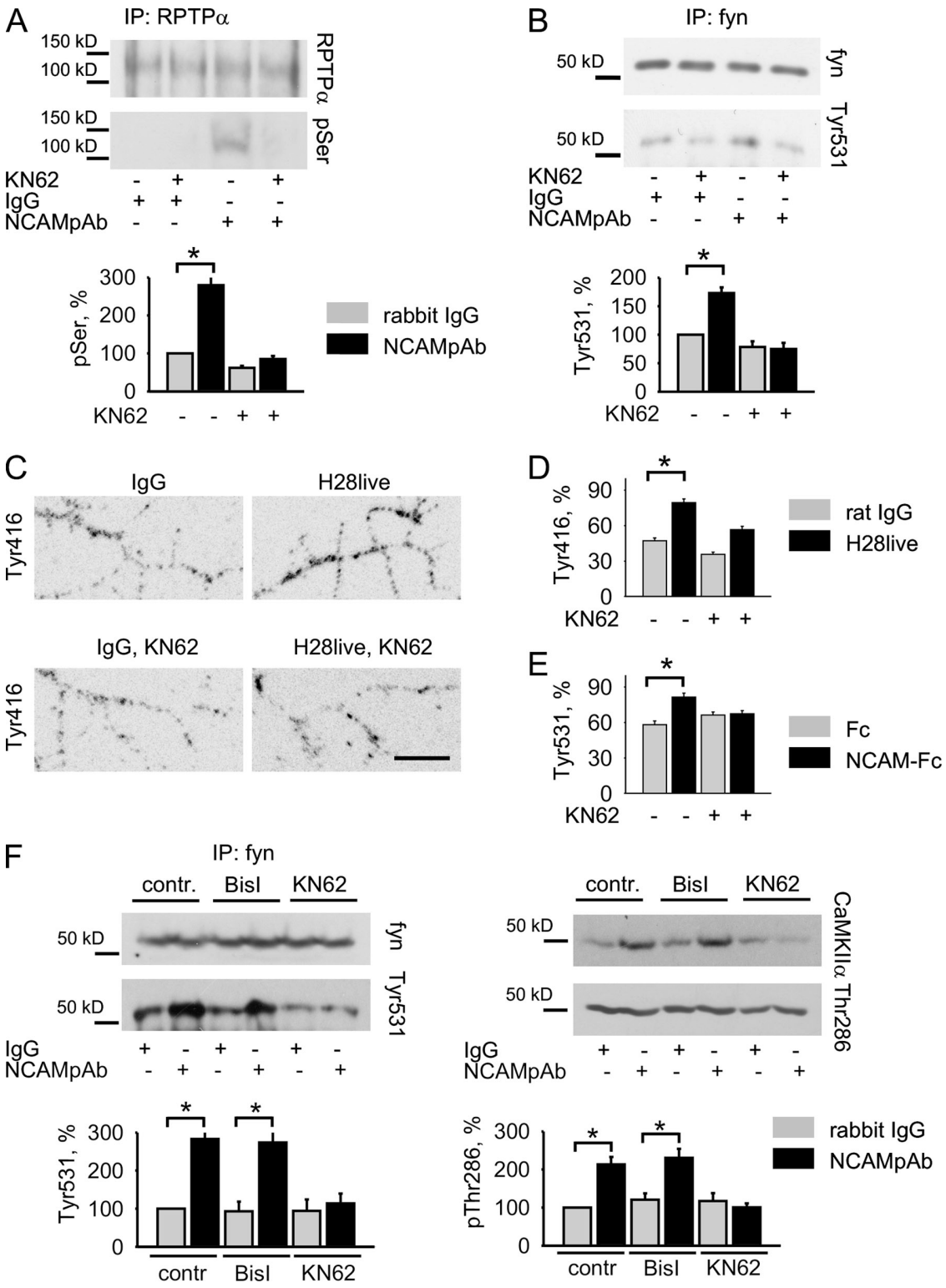

Figure 5. **CaMKIIα activity is required for NCAM140-induced fyn activation.** (A and B) CHO cells were cotransfected with NCAM140 and RPTPαWT and treated with nonspecific rabbit IgG or NCAM polyclonal antibodies in the absence or presence of KN62. RPTPα and fyn immunoprecipitates from the lysates of these cells were then probed with phosphoserine antibodies (A) or antibodies against activated Tyr531-dephosphorylated fyn (B) by Western blotting. Note that similar levels of RPTPα and fyn were immunoprecipitated in all groups. KN62 inhibited serine phosphorylation of RPTPα and activation of fyn in response to NCAM antibodies. Graphs show quantitation of the blots (mean ± SEM), with the levels in cells treated with nonspecific IgG without KN62 set to 100%. (C) Representative images of neurites of cultured hippocampal neurons treated with nonspecific rat IgG or NCAM monoclonal antibodies (H28live) in the presence or absence of KN62 and labeled with antibodies against activated Tyr416-phosphorylated fyn by indirect immunofluorescence. Inverted immunofluorescence images are shown to accentuate the differences in labeling intensities. Note the higher levels of activated fyn along neurites of NCAM antibody-treated neurons and the inhibition of this effect by KN62. Bar, 10 µm. (D and E) Graphs show mean levels ± SEM in arbitrary units of active Tyr416-phosphorylated (D) or Tyr531-dephosphorylated (E) fyn along neurites of hippocampal neurons treated with nonspecific rat IgG or NCAM monoclonal antibodies (H28live, D), or Fc or NCAM-Fc (E) in the absence or presence of KN62. $n > 90$ neurites from 45 neurons from 3 coverslips

In agreement with this idea, NCAM140 coimmunoprecipitated with CaMKIIα from brain lysates (Fig. 3 D). NCAM180 also coimmunoprecipitated with CaMKIIα (Fig. 3 D), in accordance with our previously published data (Sytnyk et al., 2006). It is interesting in this respect that clustering of NCAM140 induced activation of both CaMKIIα and RPTPα (Figs. 1 and S2, available at http://www.jcb.org/cgi/content/full/jcb.200803045/DC1), whereas clustering of NCAM180 induced activation of CaMKIIα but not RPTPα (Figs. S1 and S2). The intracellular domain of NCAM140 binds to the intracellular domain of RPTPα with higher affinity than the intracellular domain of NCAM180 in in vitro binding assays (Bodrikov et al., 2005). Furthermore, only NCAM140 but not NCAM180 associates with RPTPα in transfected CHO cells (Bodrikov et al., 2005). Collectively, previous observations and our new data suggest that the tight association of NCAM140 with RPTPα is required for CaMKIIα-mediated serine phosphorylation of RPTPα.

CaMKIIα phosphorylates the intracellular domain of RPTPα and increases its phosphatase activity

To directly analyze the CaMKIIα-mediated serine phosphorylation of RPTPα, recombinant intracellular domains of RPTPα (RPTPα-ID) were used in an in vitro phosphorylation assay: incubation of RPTPα-ID with recombinant CaMKIIα resulted in a pronounced increase in serine phosphorylation and phosphatase activity of RPTPα-ID (Fig. 4 A).

Next, we verified whether CaMKIIα also phosphorylates endogenous full-length RPTPα, which was immunopurified from NCAM−/− brain lysates to assure that serine phosphorylation of RPTPα was not saturated. Incubation of RPTPα with recombinant CaMKIIα resulted in RPTPα phosphorylation (Fig. 4 B). Similarly, RPTPα was phosphorylated by CaMKIIα immunopurified from rat brain and used instead of recombinant CaMKIIα (unpublished data). Bisindolylmaleimide I (BisI), an inhibitor of PKC isozymes, among them PKCδ, had no effect on RPTPα phosphorylation in these experiments (Fig. 4 B), which excluded the possibility that RPTPα was phosphorylated by PKCδ copurified with RPTPα from brain lysates. Phosphorylation of RPTPα by recombinant CaMKIIα was blocked in the presence of KN62, an inhibitor of CaMKIIα (Fig. 4 B).

To analyze the sites of CaMKIIα-mediated phosphorylation, RPTPαWT and RPTPαS180A, RPTPαS204A, and RPTPαS180/204A mutants were transfected into RPTPα-negative fibroblasts. Transfected proteins were then immunoisolated from cell lysates and incubated with recombinant CaMKIIα. Incubation with CaMKIIα resulted in an approximately sixfold increase in serine phosphorylation of RPTPαWT, whereas CaMKIIα-mediated serine phosphorylation of RPTPαS180A and RPTPαS204A was reduced and serine phosphorylation of RPTPαS180/204A was fully blocked (Fig. 4 C). The levels of serine phosphorylation of RPTPα induced by CaMKIIα correlated with the levels of RPTPα phosphatase activity after incubation with CaMKIIα: the highest increase in the phosphatase activity was observed for RPTPαWT, being lower for RPTPαS180A and RPTPαS204A, whereas it was not detectable for RPTPαS180/204A (Fig. 4 C). Interestingly, mutation of Ser180 had a more profound effect on CaMKIIα-induced serine phosphorylation and phosphatase activity of RPTPα than the Ser204 mutation (Fig. 4 C), which correlates with the effect of these mutations on NCAM-induced RPTPα phosphorylation (Fig. 1). We conclude that CaMKIIα phosphorylates RPTPα at Ser180 and Ser204.

CaMKIIα is required for NCAM-induced fyn activation

To confirm that NCAM140-induced serine phosphorylation of RPTPα is mediated by CaMKIIα in live cells, CHO cells were cotransfected with NCAM140 and RPTPαWT and treated with NCAM antibodies in the absence or presence of the CaMKIIα inhibitor KN62. Application of NCAM antibodies strongly increased serine phosphorylation of RPTPαWT in transfected cells, as measured by Western blotting with phosphoserine-specific antibodies (Fig. 5 A). NCAM-dependent serine phosphorylation of RPTPαWT was inhibited by KN62 (Fig. 5 A), which indicates that CaMKIIα activation is required for NCAM-induced RPTPα phosphorylation.

Because RPTPα is the major phosphatase that induces fyn activation in NCAM-activated signaling (Bodrikov et al., 2005), we analyzed whether CaMKIIα activity is required for fyn activation in response to NCAM clustering at the cell surface. Application of NCAM antibodies to CHO cells cotransfected with NCAM140 and RPTPαWT increased levels of Tyr531-dephosphorylated and thus activated fyn in these cells, as measured by Western blot analysis (Fig. 5 B). NCAM-induced fyn activation was completely inhibited by KN62 (Fig. 5 B).

Similarly, KN62 inhibited fyn activation in response to application of NCAM antibodies or NCAM-Fc to cultured neurons as shown by immunofluorescence labeling or Western blot analysis of active fyn with antibodies specific for Tyr531-dephosphorylated or Tyr416-autophosphorylated fyn (Fig. 5, C–F). The PKCδ inhibitor BisI had no effect on NCAM-induced fyn activation (Fig. 5 F). Thus, we conclude that CaMKIIα activity is required for NCAM-induced RPTPα-mediated fyn activation.

Association of NCAM with lipid rafts is required for NCAM-induced CaMKIIα activation

Clustering of NCAM140 and NCAM180 induces their redistribution to lipid rafts (Niethammer et al., 2002; Leshchyns'ka et al., 2003; Bodrikov et al., 2005; Santuccione et al., 2005). Therefore, we analyzed whether lipid rafts play a role in NCAM-induced CaMKIIα activation. In cultured hippocampal neurons extracted with cold 1% Triton X-100 and colabeled with antibodies against Thr286-phosphorylated CaMKIIα and the lipid raft marker PI(4,5)

analyzed in each group (for D and E). (F) Cultured cortical neurons were treated with nonspecific rabbit IgG or NCAM polyclonal antibodies in the absence or presence of BisI and KN62. Lysates of these cells and fyn immunoprecipitates from the lysates were then probed with the indicated antibodies by Western blotting. Note that KN62 but not BisI inhibited fyn and CaMKIIα activation in response to NCAM antibodies. Graphs show quantitation of the blots (mean ± SEM) with the levels in cells treated, with nonspecific IgG without inhibitors set to 100%. *, $P < 0.05$ (paired *t* test).

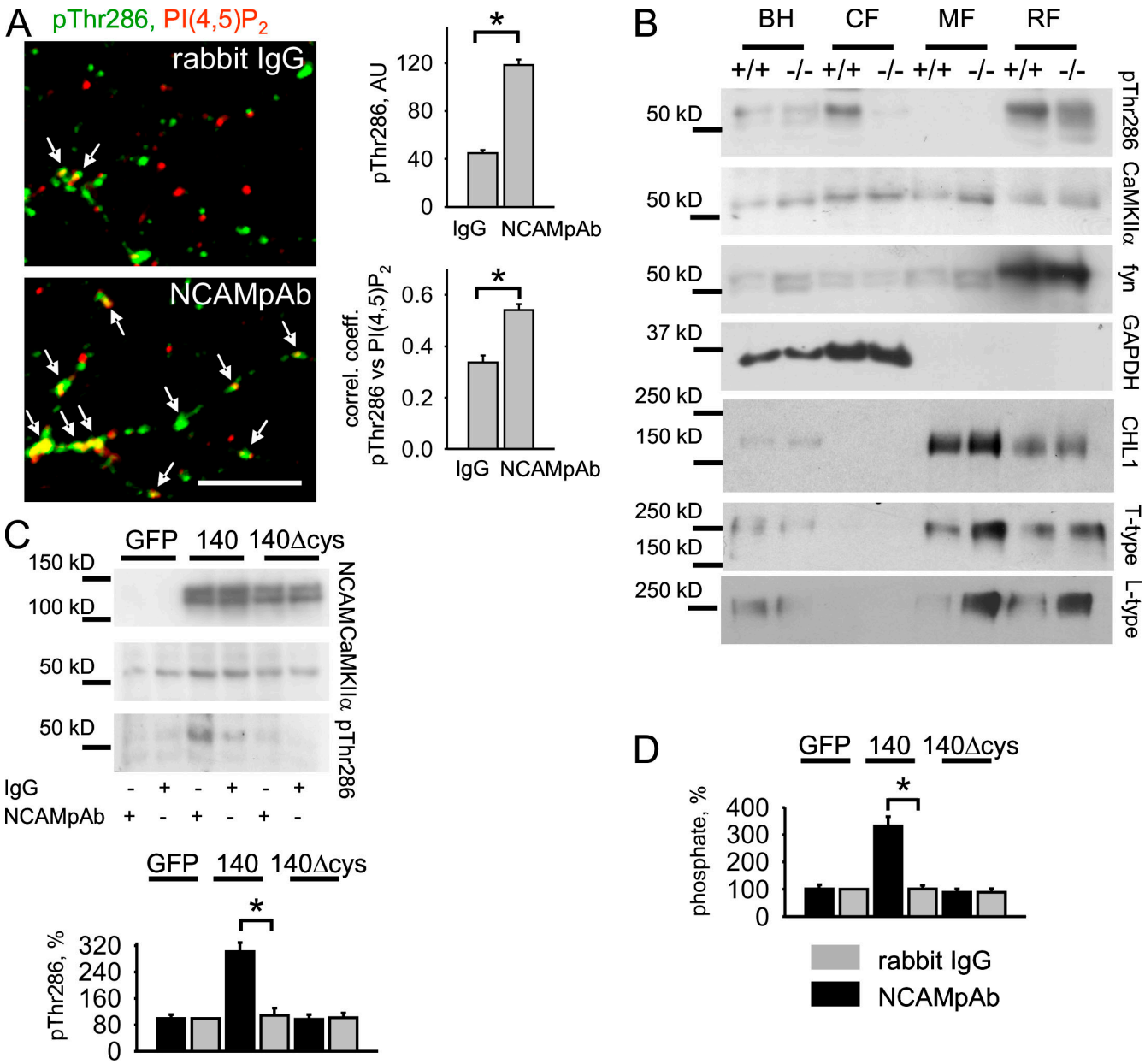

Figure 6. **Association of NCAM140 with lipid rafts is required for CaMKIIα activation.** (A, left) Representative images of neurites of cultured hippocampal neurons treated with nonspecific rabbit IgG or NCAM polyclonal antibodies, extracted in cold 1% Triton X-100, and labeled with antibodies against activated Thr286-phosphorylated CaMKIIα and PI(4,5)P2 by indirect immunofluorescence. Note the higher levels of activated CaMKIIα and the higher degree of colocalization of activated CaMKIIα with $PI(4,5)P_2$ along neurites of NCAM antibody-treated neurons. Arrows show clusters of activated CaMKIIα co-localizing with $PI(4,5)P_2$ accumulations. Bar, 10 µm. (right) Graphs show mean levels ± SEM in arbitrary units (AU) of active Thr286-phosphorylated CaMKIIα (top) and coefficients of correlation between distributions of Thr286 phosphorylated CaMKIIα and $PI(4,5)P_2$ (bottom) along neurites. $n > 90$ neurites from 45 neurons from 3 coverslips analyzed in each group. (B) Brain homogenates (BH), cytosolic fraction (CF), total membrane fraction (MF), and lipid raft fraction (RF) from NCAM+/+ and NCAM−/− brains were probed by Western blotting with antibodies against activated Thr286 phosphorylated CaMKIIα, total CaMKIIα, T- and L-type VDCC, lipid raft marker fyn, the soluble protein marker GAPDH, and the membrane protein marker CHL1. Note the accumulation of activated CaMKIIα in lipid rafts. (C) Lysates of CHO cells cotransfected with RPTPαWT and NCAM140, NCAM140Δcys, or GFP and treated with nonspecific rabbit IgG or NCAM polyclonal antibodies were probed with antibodies against NCAM, activated Thr286-phosphorylated CaMKIIα, and total CaMKIIα. Note the similar levels of expression of NCAM140 and NCAM140Δcys but the reduced activation of CaMKIIα in NCAM140Δcys- versus NCAM140-transfected cells. The graph shows quantitation of the blots with the levels of activated CaMKIIα in GFP-transfected cells treated with nonspecific IgG set to 100%. (D) RPTPα was immunoprecipitated from cell lysates in C, and serine phosphorylation of RPTPα was analyzed by alkaline hydrolysis. The amount of phosphate released by alkaline hydrolysis from RPTPα from cells transfected with GFP instead of NCAM and treated with nonspecific IgG was set to 100%. For C and D, mean values ± SEM are shown ($n = 6$). *, $P < 0.05$ (paired t test).

P2 (Niethammer et al., 2002), accumulations of activated CaMKIIα partially overlapped with the clusters of PI(4,5)P2 (Fig. 6 A), which indicates that cytoskeleton- and/or lipid raft–associated detergent-insoluble pools of CaMKIIα were present in neurites. Clustering of NCAM at the cell surface with NCAM antibodies resulted in an approximately threefold increase in the levels of detergent-insoluble active CaMKIIα and a higher overlap in distribution of CaMKIIα and PI(4,5)P2 along neurites when compared with

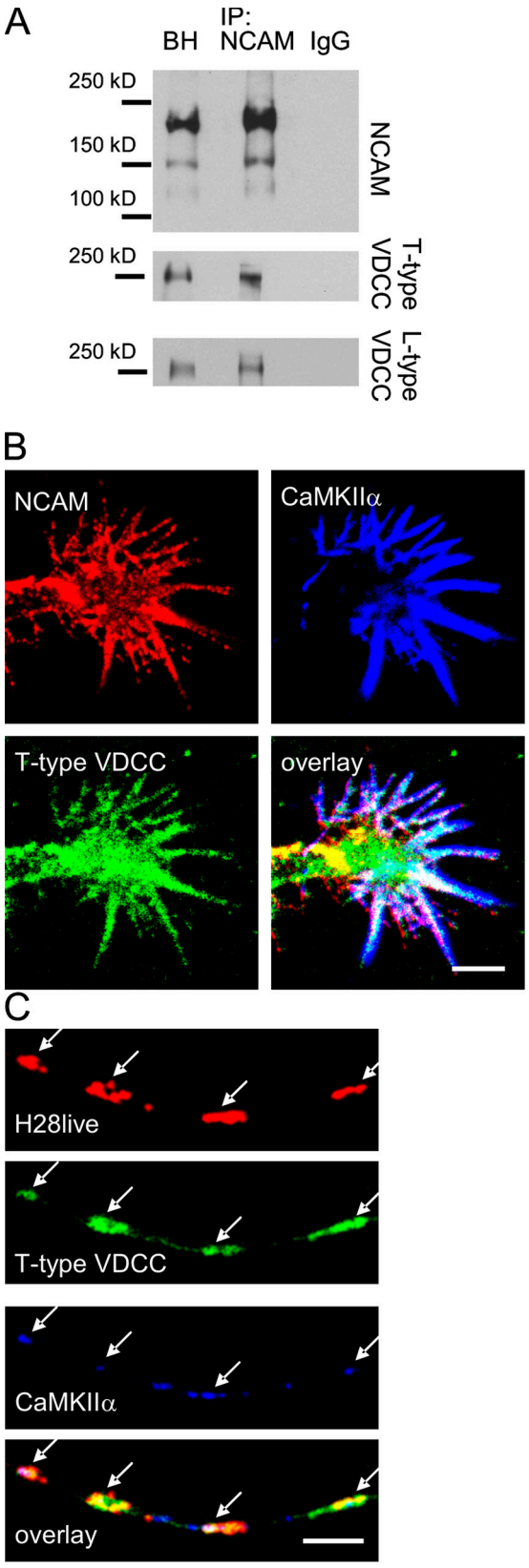

Figure 7. **NCAM associates with T- and L-type VDCC.** (A) NCAM immunoprecipitates (IP) from NCAM+/+ brain lysates were analyzed by Western blotting with antibodies against NCAM and T- and L-type VDCC. Mock immunoprecipitation with nonspecific IgG served as control. Brain homogenate (BH) is shown for comparison. T- and L-type VDCC coimmunoprecipitate with NCAM. (B) A growth cone of a cultured hippocampal neuron colabeled with antibodies against NCAM, CaMKIIα, and T-type VDCC is shown. Note the colocalization of these three proteins in filopodia. (C) NCAM was clustered at the surface of cultured hippocampal neurons with NCAM monoclonal antibodies (H28live), and neurons were colabeled with antibodies against CaMKIIα and T-type VDCC. A representative neurite is shown. Note that clusters of NCAM overlap with accumulations of T-type VDCC and CaMKIIα (arrows). Bars, 5 μm.

neurons treated with nonspecific immunoglobulins (Fig. 6 A). This observation suggests that activation of CaMKIIα in response to NCAM clustering occurs in lipid rafts.

In agreement, Western blot analysis of the cytosolic, total membrane, and lipid raft fractions isolated from the brain tissue of young mice showed that activated CaMKIIα accumulated in lipid rafts (Fig. 6 B). In contrast, total CaMKIIα protein was broadly distributed in all fractions (Fig. 6 B). Importantly, levels of activated CaMKIIα but not total CaMKIIα protein, fyn, or glyceraldehyde-3-phosphate dehydrogenase (GAPDH) were reduced in the cytosolic fraction and lipid rafts from NCAM−/− versus NCAM+/+ brains (Figs. 6 B and S3, available at http://www.jcb.org/cgi/content/full/jcb.200803045/DC1), which indicates that NCAM is implicated in the activation of CaMKIIα that accumulates in lipid rafts and/or redistributes to the soluble pool.

To analyze whether redistribution of NCAM to lipid rafts is required for CaMKIIα activation and RPTPα phosphorylation, CHO cells were cotransfected with RPTPαWT and NCAM140 or NCAM140ΔCys, an NCAM140 mutant with inactivated palmitoylation sites within its intracellular domain that blocks its association with lipid rafts (Niethammer et al., 2002). Application of NCAM antibodies to NCAM140-transfected cells resulted in a pronounced increase in the levels of activated CaMKIIα and serine phosphorylation of RPTPαWT in these cells (Fig. 6, C and D). Although expression levels of NCAM140ΔCys were similar to those of NCAM140, application of NCAM antibodies did not influence levels of activated CaMKIIα and phosphorylated RPTPαWT in NCAM140ΔCys-transfected cells nor in GFP-transfected cells used as a negative control (Fig. 6, C and D). NCAM140-dependent CaMKIIα activation and RPTPα phosphorylation and activation were also blocked in CHO cells treated with methyl-β-cyclodextrin (Fig. S3), an agent that binds to cholesterol, thereby destroying the integrity of lipid rafts (Niethammer et al., 2002). Thus, association of NCAM with lipid rafts is required for NCAM-dependent CaMKIIα activation and RPTPα phosphorylation.

NCAM associates with T- and L-type voltage-dependent Ca^{2+} channels (VDCC)

CaMKIIα activation depends on an increase in cytosolic Ca^{2+} that binds to CaM. Binding of Ca^{2+}-CaM to the regulatory domain of the kinase activates the kinase by releasing the catalytic domain from inhibition by autoregulatory sequences proximal to the CaM binding site. NCAM clustering at the cell surface has been shown to be accompanied by an increase in Ca^{2+} concentration in the cytosol, with the VDCC of the T and, to a lower extent, L type playing a major role in NCAM-dependent Ca^{2+} influx to the cell (Schuch et al., 1989; Kiryushko et al., 2006). T- and L-type VDCC were present at high levels in lipid rafts from brain tissue (Fig. 6 B), thus they are well poised to provide Ca^{2+} for

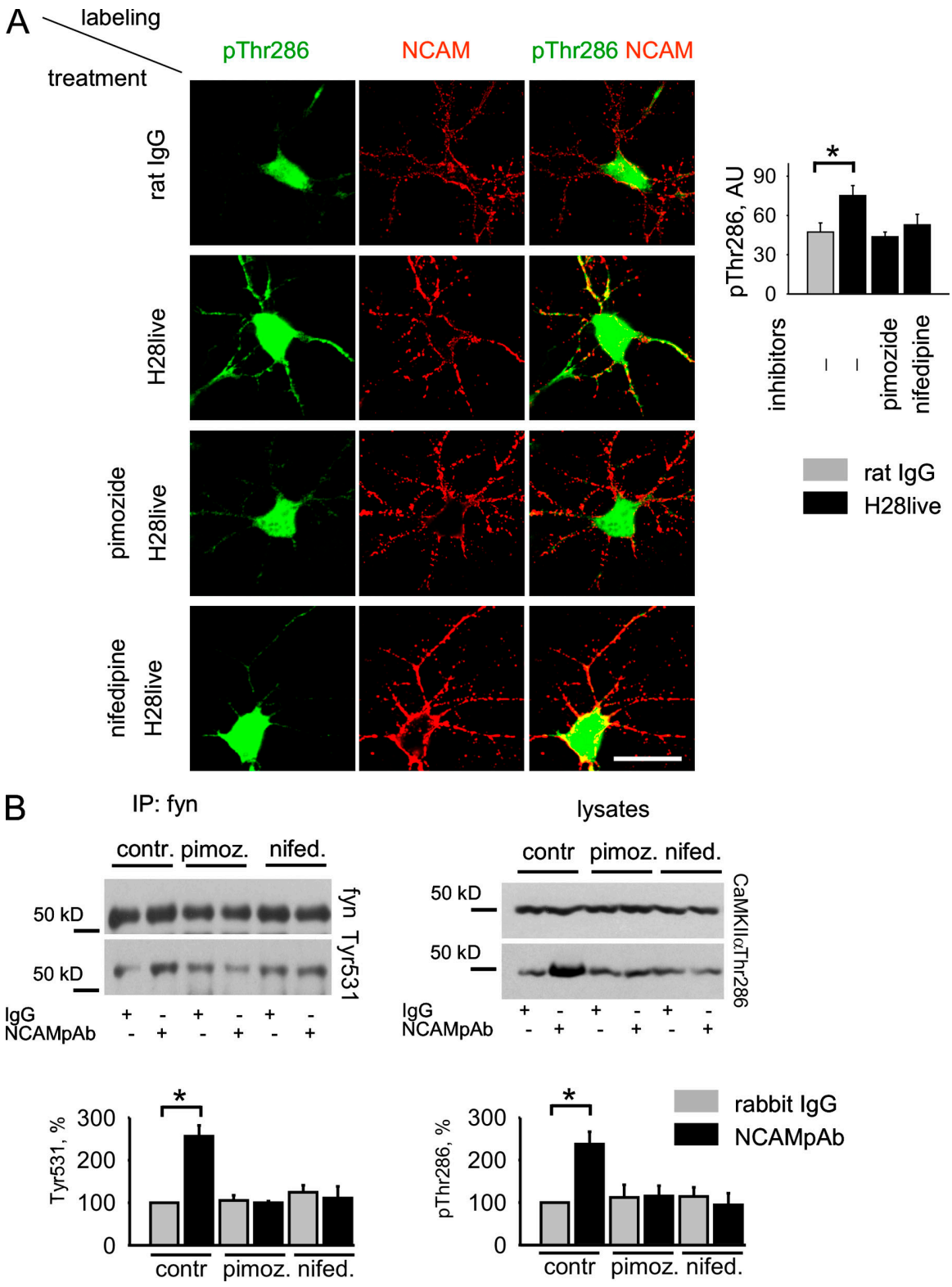

Figure 8. **NCAM-induced CaMKIIα activation depends on Ca^{2+} influx via T- and L-type VDCC.** (A) Cultured hippocampal neurons were incubated with pimozide and nifedipine, inhibitors of T-and L-type VDCC, respectively. Neurons were then stimulated with rat NCAM monoclonal antibodies (H28live) or nonspecific rat IgG, then fixed and colabeled with antibodies against activated Thr286-phosphorylated CaMKIIα. Representative images are shown. Note that clustering of NCAM without inhibitors induces an increase in active CaMKIIα levels along neurites and that active CaMKIIα accumulates in NCAM clusters. Pimozide and nifedipine inhibit CaMKIIα activation. Graph shows mean levels ± SEM in arbitrary units (AU) of active CaMKIIα along neurites. $n > 45$ neurites from 30 neurons from 3 coverslips analyzed in each group. Bar, 20 µm. (B) Cultured cortical neurons were treated with nonspecific rabbit IgG or NCAM polyclonal antibodies in the absence or presence of pimozide and nifedipine. Lysates of these cells and fyn immunoprecipitates from the lysates were then probed with the indicated antibodies by Western blotting. Note that pimozide and nifedipine inhibited fyn and CaMKIIα activation in response to NCAM antibodies. Graphs show quantitation of the blots (mean ± SEM), with the levels in cells treated with nonspecific IgG without inhibitors set to 100%. *, $P < 0.05$ (paired *t* test).

CaMKIIα activation in response to NCAM redistribution to lipid rafts. Moreover, T- and L-type VDCC associated with NCAM in the brain, as shown by coimmunoprecipitation of these VDCC with NCAM from brain lysates (Fig. 7 A). Although L-type VDCC are known to accumulate in growth cones being involved in cytoskeleton rearrangements (Ohbayashi et al., 1998), much less is known about T-type VDCC. Colabeling of cultured hippocampal neurons with antibodies against NCAM, T-type VDCC, and CaMKIIα showed that all three proteins accumulated in growth cones and, in particular, growth cone filopodia (Fig. 7 B). When NCAM was clustered at the neuronal surface with NCAM antibodies, T-type VDCC and CaMKIIα accumulated in NCAM clusters along neurites (Fig. 7 C). Thus, we hypothesize that clustering of NCAM at the growth cones induces formation of the NCAM–T- and L-type VDCC–CaMKIIα complex, thereby linking CaMKIIα to the Ca^{2+} source.

NCAM-induced CaMKIIα activation depends on Ca^{2+} influx via T- and L-type VDCC

Next, we verified the role of T- and L-type VDCC in NCAM-dependent CaMKIIα activation. In cultured hippocampal neurons, clustering of NCAM at the neuronal surface induced an ~80% increase in the levels of activated Thr286-phosphorylated CaMKIIα along neurites, as shown by immunocytochemical analysis (Fig. 8 A). Pimozide, a T-type VDCC inhibitor, completely blocked this effect (Fig. 8 A). Nifedipine, an L-type VDCC inhibitor, also inhibited NCAM-dependent CaMKIIα activation, although with a slightly lower efficiency than pimozide (Fig. 8 A).

Similarly, pimozide and nifedipine inhibited NCAM-dependent CaMKIIα activation in cultured cortical neurons analyzed by Western blotting (Fig. 8 B). Importantly, pimozide and nifedipine also blocked NCAM-dependent dephosphorylation of fyn at Tyr531 (Fig. 8 B). Hence, we conclude that NCAM induces Ca^{2+} influx via T- and L-type VDCC for CaMKIIα activation, which results in up-regulation of the phosphatase activity of RPTPα and fyn dephosphorylation and activation.

Phosphorylation of RPTPα on Ser180 and Ser204 is required for NCAM-mediated neurite outgrowth

In neurons exposed to NCAM-Fc in the culture medium (Fig. 9 A) or seeded on top of NCAM-transfected fibroblasts (Williams et al., 1995), the KN62 inhibitor of CaMKIIα abolished the NCAM-dependent increase in neurite outgrowth over the baseline level of nonstimulated neurons, which indicates that CaMKIIα activity is required for NCAM-mediated neurite outgrowth.

To analyze whether CaMKIIα-dependent RPTPα phosphorylation on Ser180 and/or Ser204 is required for NCAM-mediated neurite outgrowth, cultured neurons were transfected with GFP or cotransfected with GFP and RPTPαWT or the RPTPα mutants RPTPαS180A, RPTPαS204A, or RPTPαS180/204A. These mutations within RPTPα did not affect binding of RPTPα to NCAM (Fig. 1). Hence, RPTPα mutants overexpressed in neurons should act in a dominant-negative fashion by substituting for endogenous RPTPα in the NCAM–RPTPα complex. Overexpression of RPTPαWT in neurons resulted in enhanced neurite outgrowth most likely caused by the nonspecific outgrowth-promoting activation of Src-family kinases by RPTPαWT (Fig. 9 B). Exposure of GFP-transfected neurons to NCAM-Fc applied in the culture medium increased neurite lengths by ~100% when compared with Fc-treated GFP-transfected control neurons (Fig. 9 B). A similar, ~100% increase in neurite length was observed for NCAM-Fc–versus Fc-treated RPTPαWT-transfected neurons (Fig. 9 B). However, neurites in NCAM-Fc–treated RPTPαWT-transfected neurons were approximately two times longer than in NCAM-Fc–treated GFP-transfected neurons, which indicates that RPTPαWT potentiates the response to NCAM-Fc (Fig. 9 B). RPTPαS180A and RPTPαS204A mutants showed a reduced ability to promote neurite outgrowth and to enhance responsiveness to NCAM-Fc when compared with RPTPαWT (Fig. 9 B). The RPTPαS180A mutant was strongly impaired in its ability to nonspecifically promote neurite outgrowth but did not completely block the response to NCAM-Fc. In contrast, the RPTPαS204A mutant strongly interfered with the response to NCAM-Fc but was still able to nonspecifically promote neurite outgrowth at a level that was not different from that of RPTPαWT. A plausible explanation for this observation is that Ser180 and Ser204 may play slightly distinct roles in the maintenance of the unregulated basal versus the NCAM-mediated, thus

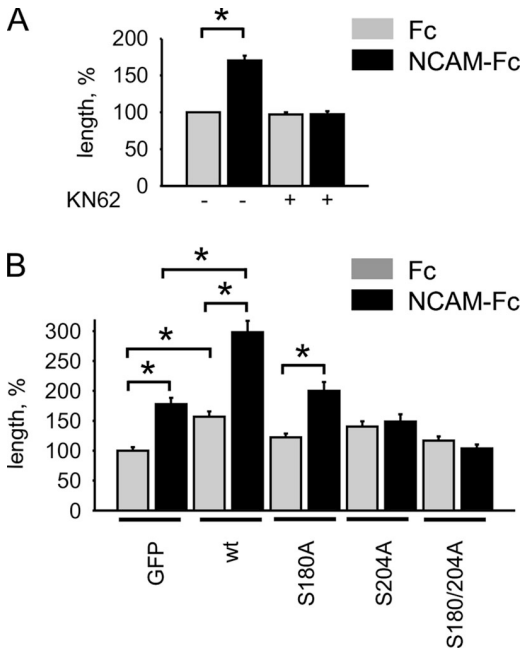

Figure 9. **NCAM-induced phosphorylation of RPTPα on Ser180 and Ser204 is required for NCAM-mediated neurite outgrowth.** (A) Cultured hippocampal neurons were treated with Fc or NCAM-Fc in the presence or absence of KN62. Graph shows mean lengths of neurites ± SEM normalized to the mean neurite length in neurons treated with Fc in the absence of KN62 (n > 200). Note that KN62 inhibits NCAM-dependent neurite outgrowth. (B) Cultured hippocampal neurons were transfected with GFP alone or cotransfected with GFP and RPTPαWT or RPTPα mutants and treated with Fc or NCAM-Fc. Graph shows mean lengths of neurites ± SEM normalized to the mean neurite length in Fc-treated GFP-transfected neurons (n > 150). Note that RPTPαWT promotes neurite outgrowth and potentiates the response to NCAM-Fc. Mutation in either Ser180 or Ser204 inhibits the outgrowth-promoting effect of RPTPα, whereas the RPTPαS180/204A mutant functions as a dominant-negative construct that fully blocks NCAM-dependent neurite outgrowth. *, $P < 0.05$ (t test).

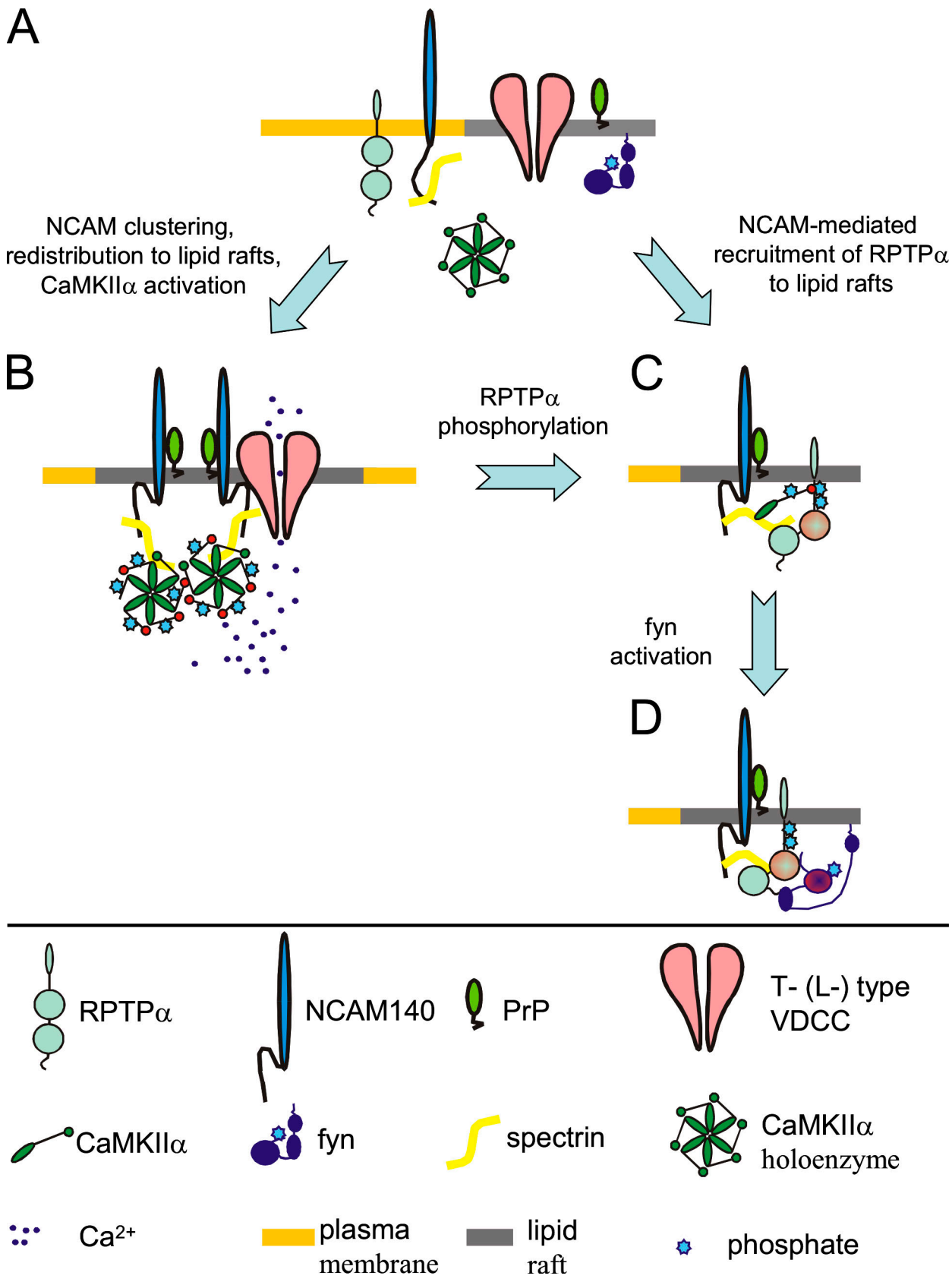

Figure 10. **A schematic model of molecular interactions induced by NCAM140 clustering and resulting in fyn activation.** (A) Nonclustered NCAM140 resides outside of lipid rafts and does not associate with RPTPα, CaMKIIα (shown as a holoenzyme), and fyn, which are present in inactive forms in the plasma membrane outside of lipid rafts, in the cytosol and in lipid rafts, respectively. (B) NCAM140 clustering induces palmitoylation of the intracellular domain of NCAM140 that promotes NCAM140 redistribution to lipid rafts, where it binds to prion protein (PrP). In parallel, NCAM140 clustering induces FGFR activation, promoting arachidonic acid production (not depicted), which results in arachidonic acid–dependent Ca^{2+} influx (Williams et al., 1994)

regulated, neurite outgrowth. A double mutant RPTPαS180/204 did not promote neurite outgrowth and totally blocked the NCAM-Fc–induced response (Fig. 9 B). Thus, we conclude that CaMKIIα-mediated phosphorylation of Ser180 and Ser204 within the RPTPα intracellular domain is required for NCAM-induced neurite outgrowth.

Discussion

In this study, we have further explored the cascades of molecular interactions activated by the neural cell adhesion molecule NCAM; the molecular players in the functional interconnection had been previously implicated in NCAM-dependent neurite outgrowth. The tyrosine kinase fyn was the first to be identified as an NCAM-associated signaling partner that triggers the MAP kinase/FAK-related downstream signaling of NCAM, leading to activation of transcription factors, such as CREB (Beggs et al., 1997; Schmid et al., 1999; Jessen et al., 2001). The fyn pathway then became very important as a cosignaling pathway in NCAM-induced signaling, which needed to be activated in lipid rafts in parallel with the FGF receptor located outside of lipid rafts in order to trigger converging signaling cascades to enhance neurite outgrowth (Niethammer et al., 2002). Because the intracellular domain of NCAM does not contain sequences known to induce fyn activation, we previously investigated the relationship between NCAM and the well-known activator of Src-family tyrosine kinases, of which fyn is a member, the receptor protein tyrosine phosphatase RPTPα. RPTPα that dephosphorylates Tyr-531 of fyn to activate the enzyme (Bhandari et al., 1998) is highly enriched in neurons and growth cones (Helmke et al., 1998), where it colocalizes with NCAM (Bodrikov et al., 2005). We identified RPTPα as a direct binding partner of NCAM140, linking this NCAM isoform to fyn. Interestingly, the interaction between NCAM and RPTPα was enhanced by spectrin (Bodrikov et al., 2005), which also interacts directly with the intracellular domains of the transmembrane isoforms of NCAM, NCAM140, and, in particular, NCAM180 (Pollerberg et al., 1986, 1987; Sytnyk et al., 2002; Leshchyns'ka et al., 2003) and indirectly via lipid rafts with the GPI-anchored isoform NCAM120 (Leshchyns'ka et al., 2003).

In this study, we expand our previous findings by showing that clustering of NCAM at the cell surface enhances serine phosphorylation and phosphatase activity of RPTPα, thus identifying NCAM as the first recognition molecule and surface receptor that not only associates with but also regulates the catalytic activity of RPTPα. The catalytic phosphatase activity of RPTPα can be enhanced by PKC-mediated Ser180 and/or Ser204 phosphorylation of the intracellular domain of RPTPα (den Hertog et al., 1995; Tracy et al., 1995; Stetak et al., 2001; Zheng et al., 2002), with PKCδ but not other PKC isoforms playing the major role in the phosphorylation of RPTPα on Ser180 and Ser204 (Brandt et al., 2003). However, we found that PKCδ is not involved in NCAM-induced activation. In agreement with this notion is the observation that 2.5–10 μM of the PKCδ inhibitor rottlerin did not inhibit RPTPα serine phosphorylation in nonstimulated NIH3T3 fibroblasts, and that very high concentrations of rottlerin (50 μM) only mildly affected RPTPα serine phosphorylation (unpublished data), which suggests that other enzymes are involved. Furthermore, we show that BisI, a PKCδ inhibitor, does not block RPTPα-mediated fyn activation in response to NCAM clustering. Accordingly, we identified CaMKIIα as a previously unrecognized enzyme that binds to and phosphorylates RPTPα at serine residues Ser180 and Ser204, increasing the phosphatase activity of RPTPα. We also show that CaMKIIα, which associates with NCAM via spectrin (Sytnyk et al., 2006), is activated in response to clustering of NCAM at the cell surface. Calmodulin, which associates with RPTPα in the presence of Ca^{2+}, may thus play a role in CaMKIIα activation (Liang et al., 2000). NCAM-induced CaMKIIα activation then leads to phosphorylation of RPTPα at Ser180 and Ser204, which, in turn, leads to activation of lipid raft-enriched fyn (Fig. 10).

Overexpression of RPTPα in neurons enhances basal neurite outgrowth rates, probably by nonspecific activation of Src-family kinases. Indeed, overexpression of RPTPα in nonneuronal cells results in persistent activation of Src, with concomitant cell transformation and tumorigenesis (Zheng et al., 1992, 2000), and mutation of Ser180 or Ser204 blocks neoplastic transformation of cells by RPTPα (Zheng et al., 2002). This suggests that phosphorylation and activity of RPTPα are tightly regulated in normal cells. Homeostatic mechanisms that coordinate changes in RPTPα phosphatase activity are therefore intimately linked with the changes in cell behavior. It is thus not surprising that disturbance of the relationship of NCAM with RPTPα may link NCAM to tumorigenesis in different cell types that express NCAM (Cavallaro and Christofori, 2004a,b).

Our study again emphasizes the importance of lipid-enriched microdomains, the so-called lipid rafts. The fact that NCAM uses this signaling platform for fyn activation has previously been shown by ablating the palmitoylation sites in the intracellular domain of NCAM, which target the two major transmembrane isoforms of NCAM to lipid rafts (Niethammer et al., 2002). NCAM-dependent fyn activation was also reduced in prion protein-deficient mice, which correlates with reduced levels of NCAM in lipid rafts isolated from these mice and implicates prion protein as a lipid raft–recruiting signal for NCAM (Santuccione et al., 2005). In this study, we provide further details on the molecular interactions induced by NCAM in lipid rafts by showing that if the targeting of NCAM140 to lipid rafts

via T- and L-type VDCC. An increase in Ca^{2+} concentration promotes binding of Ca^{2+}/CaM to CaMKIIα, releasing the catalytic domain of CaMKIIα from inhibition by autoregulatory sequences proximal to the CaM binding site (not depicted). By associating with T- and L-type VDCC, NCAM anchors CaMKIIα, which is bound to NCAM140 via spectrin, near the Ca^{2+} influx sites. NCAM-induced aggregation of CaMKIIα in lipid rafts promotes transautophosphorylation of the CaMKIIα holoenzymes at Thr286, resulting in the constitutive activation of CaMKIIα. (C) In parallel to CaMKIIα activation, NCAM140 promotes redistribution of RPTPα to lipid rafts. In lipid rafts, activated CaMKIIα (only one CaMKIIα molecule is shown for simplicity) phosphorylates RPTPα at Ser180 and Ser204, which changes the conformation of RPTPα, resulting in enzyme activation. (D) Activated RPTPα binds and dephosphorylates fyn at Tyr531, activating the enzyme. Downstream targets of active fyn include the Ras–MAP (MAP) kinase pathway, the sustained activity of which is required for neuronal differentiation (not depicted).

is disturbed, NCAM-induced activation of CaMKIIα in lipid rafts and subsequent phosphorylation and activation of RPTPα, and thus of fyn, are reduced. Because aggregation and oligomerization of CaMKIIα is necessary for full activation of the enzyme (Hudmon et al., 2005), we propose that the special environment of lipid rafts promotes oligomerization of NCAM-associated CaMKIIα to induce its full activation (Fig. 10). In agreement, clustering of NCAM increases the levels of detergent-insoluble oligomerized CaMKIIα in cultured hippocampal neurons (Sytnyk et al., 2006). Association of NCAM with T- and L-type VDCC accumulating in lipid rafts should then bring CaMKIIα into the vicinity of the sites of Ca^{2+} influx into the cell (Fig. 10). Thus, our present study confirms the importance of lipid rafts in cell signaling for neurite outgrowth. The generation of such platforms during ontogenetic development appears to be crucial for neurite outgrowth. It will be interesting to determine whether such cell adhesion molecule-mediated platforms are required for synaptic plasticity in the adult brain, which requires functional and structural modifications of synaptic membranes and associated signaling mechanisms.

Materials and methods

Antibodies and toxins

Rabbit polyclonal antibodies against NCAM (for biochemical and immunocytochemical experiments; Niethammer et al., 2002) and rat monoclonal antibodies H28 against NCAM (for immunocytochemical experiments; Gennarini et al., 1984) were against the extracellular domain of all NCAM isoforms. Rabbit antibodies against RPTPα (den Hertog et al., 1994) and CHL1 (Leshchyns'ka et al., 2006) were generated as described previously. Mouse monoclonal antibodies against PI(4,5)P2 were obtained from K. Fukami (University of Tokyo, Tokyo, Japan). Cholera toxin B subunit tagged with biotin to label GM1, rabbit polyclonal antibodies against the HA tag, L-type VDCC (α_{1C} subunit), T-type VDCC (α_{1H} subunit), and CaMKIIα were obtained from Sigma-Aldrich. Rabbit polyclonal and mouse monoclonal antibodies against $p59^{fyn}$ protein were obtained from Santa Cruz Biotechnology, Inc. Rabbit polyclonal antibodies against Tyr527-dephosphorylated or Tyr416-phosphorylated $pp60^{c\text{-}Src}$ kinase that cross-react with Tyr531-dephosphorylated or Tyr420-phosphorylated $p59^{fyn}$, against Thr505-phosphorylated PKCδ, and against Thr286-phosphorylated CaMKIIα were obtained from Cell Signaling Technology. Mouse monoclonal antibodies recognizing phosphorylated serine residues were obtained from QIAGEN, mouse monoclonal antibodies against PKCδ were obtained from BD Biosciences, rat monoclonal antibodies against GAPDH were obtained from Millipore, and mouse monoclonal antibodies against CaMKIIα were obtained from Assay Designs. Secondary antibodies against rabbit, rat, and mouse Ig coupled to HRP, Cy2, Cy3, or Cy5; and nonspecific rabbit, rat, and mouse immunoglobulins (IgG) were obtained from Dianova (Hamburg, Germany).

Animals

Wild-type 0–4-d-old C57BL/6J mice were used and compared when indicated to age-matched NCAM−/− mice provided by H. Cremer (Developmental Biology Institute of Marseille, Marseille, France; Cremer et al., 1994) and inbred for at least nine generations onto the C57BL/6J background.

Cultures of hippocampal and cortical neurons

Cultures of hippocampal neurons (for immunocytochemistry, cell ELISA, and neurite outgrowth assay) and cortical neurons (for Western blot analysis) were prepared from 1–3-d-old mice. Neurons were grown in the presence of 10% horse serum on glass coverslips coated with 100 µg/ml poly-L-lysine (Sytnyk et al., 2002, 2006).

Clustering of NCAM at the neuronal cell surface

NCAM was clustered at the neuronal surface using NCAM-Fc, rat monoclonal (clone H28), or rabbit polyclonal antibodies against the extracellular domain of NCAM. Application of these three agents produced similar levels of fyn activation in cultured neurons and fibroblasts cotransfected with NCAM140 and RPTPαWT (Figs. 5 and S4, available at http://www.jcb.org/cgi/content/full/jcb.200803045/DC1). 8 µg/ml NCAM-Fc and 8 µg/ml of human Fc, or 10 µg/ml NCAM polyclonal antibodies and 10 µg/ml nonspecific rabbit IgG were applied to live neurons in the culture medium for 10 min in a CO_2 incubator. Rat monoclonal antibodies H28 or 10 µg/ml nonimmune rat IgG were applied to live neurons for 15 min and clustered by secondary antibodies applied for 5 min, followed by washing for 5 min, all in a CO_2 incubator. We have found that with this protocol, fyn and CaMKIIα were activated within 5 min after secondary antibody application, and levels of active fyn and CaMKIIα reached a plateau within 10 min after secondary antibody application (Fig. S5). When indicated, 10 µM of the CaMKIIα inhibitor KN62 (Merck & Co., Inc.) or 0.5 µM of the PKC inhibitor BisI was applied 1 h before stimulation with antibodies or NCAM-Fc. 10 µM nifedipine and 5 µM pimozide (both from Alomone Laboratories Ltd.) were applied for 10 min before stimulation.

DNA constructs

NCAM140 and NCAM180 constructs were provided by P. Maness (University of North Carolina at Chapel Hill School of Medicine, Chapel Hill, NC). NCAM120 was provided by E. Bock (Institute of Molecular Pathology, University of Copenhagen, Copenhagen, Denmark). NCAM140Δcys was as described previously (Niethammer et al., 2002). The plasmid encoding the intracellular domain of RPTPα was a gift from C.J. Pallen (University of British Columbia, Vancouver, Canada). N-terminally HA-tagged full length RPTPα was used as described previously (den Hertog and Hunter, 1996; Blanchetot and den Hertog, 2000; Buist et al., 2000). HA-tagged RPTPαS180A, RPTPαS204A, and RPTPαS180/204A were generated by PCR-mediated site-directed mutagenesis using the following oligonucleotides: 5′-AGTCATTCCAACGCTTTCCGCCTGTCA-3′ for S180A and 5′-GCCAGGTCCCCAGCCACCAACAGGAAG-3′ for S204A. The constructs were verified by sequencing.

Neurite outgrowth assay

Neurite outgrowth was assayed as described previously (Niethammer et al., 2002). When indicated, neurons were cotransfected with GFP (Clontech Laboratories, Inc.) and wild-type or mutated RPTPα constructs 6 h after plating using Lipofectamine 2000 (Invitrogen) according to the manufacturer's instructions. For nontransfected neurons, 8 µg/ml NCAM-Fc (Chen et al., 1999) or 8 µg/ml human Fc (Dianova) were applied immediately after plating together with or without 10 µM KN62. For transfected neurons, NCAM-Fc or Fc were applied 6 h after transfection. Neurons were fixed 24 h after NCAM-Fc and Fc application. Lengths of neurites were measured using ImageJ software (National Institutes of Health).

Immunofluorescence labeling

In the indicated experiments, NCAM was clustered at the neuronal surface, with antibodies against the extracellular domain of NCAM applied to live neurons for 15 min and clustered/visualized by secondary antibodies applied for 5 min followed by washing for 5 min, all in a CO_2 incubator. In control experiments, we verified that application of nonspecific IgG does not induce NCAM clustering or redistribution of NCAM-associated proteins. When indicated, before fixation, neurons were also extracted with ice-cold 1% Triton X-100 as described previously (Bodrikov et al., 2005). Neurons were fixed in 4% formaldehyde in PBS, pH 7.3, for 15 min at room temperature, washed, permeabilized with 0.25% Triton X-100 in PBS for 5 min, and blocked in 1% BSA in PBS. For extracted neurons, the permeabilization step was omitted. Primary antibodies were applied in 1% BSA in PBS for 2 h at room temperature and detected with corresponding secondary antibodies applied for 45 min in 1% BSA in PBS at room temperature.

Image acquisition and manipulation

We used Cy2, Cy3, or Cy5 fluorochromes. Coverslips were embedded in Aqua-Poly/Mount (Polysciences, Inc.). For neurite outgrowth measurements, images of neurons were acquired at room temperature using a microscope (Axiophot 2) equipped with a digital camera (AxioCam HRc), AxioVision software (version 3.1), and a Plan-Neofluar 40× objective (numerical aperture 0.75; all from Carl Zeiss, Inc.). Immunofluorescence images were acquired at room temperature using a confocal laser scanning microscope (LSM510), LSM510 software (version 3) and an oil Plan-Neofluar 40× objective (numerical aperture 1.3; all from Carl Zeiss, Inc.) at 3× digital zoom. Contrast and brightness of the images were further adjusted in Corel Photo-Paint 9 (Corel Corporation).

Immunofluorescence quantification

Profiles of distributions of the immunofluorescence signals along neurites were obtained using ImageJ software, then used to calculate mean

immunofluorescence intensities along neurites and to analyze coefficients of correlation between distributions of the Thr286-phosphorylated CaMKIIα and PI(4,5)P2.

Cultures and transfection of CHO cells and fibroblasts

CHO cells and fibroblasts were maintained in Glasgow or Dulbecco's modified Eagle's medium, respectively, containing 10% of fetal calf serum. Cells were transfected using Lipofectamine and Plus reagent (Invitrogen) according to the manufacturer's instruction. When indicated, 10 µg/ml NCAM polyclonal antibodies or 10 µg/ml nonspecific rabbit IgG were applied to cells for 10 min. 10 µM KN62 was applied 1 h before stimulation, and NCAM antibodies were applied (as described in the Clustering of NCAM at the neuronal cell surface section) but in the presence of KN62. To deplete cholesterol from lipid rafts, cultures were incubated for 15 min with 5 mM methyl-β-cyclodextrin (MCD; Sigma-Aldrich) before stimulation, and NCAM antibodies were applied (as described in the Clustering of NCAM at the neuronal cell surface section) but in the presence of MCD. All reagents were applied in culture medium at 37°C in a CO_2 incubator.

Immunoprecipitation and coimmunoprecipitation

Brain homogenates were prepared using 50 mM Tris-HCl buffer, pH 7.5, containing 1 mM $CaCl_2$, 1 mM $MgCl_2$, and 1 mM $NaHCO_3$. Samples containing 1 mg of total protein were lysed for 40 min on ice with RIPA buffer (50 mM Tris-HCl buffer, pH 7.5, containing 150 mM NaCl, 1% Nonidet P-40, 0.5% deoxycholate, 1 mM $Na_2P_2O_7$, 1 mM NaF, 2 mM $NaVO_4$, 0.1 mM PMSF, and EDTA-free protease inhibitor cocktail [Roche]). In experiments with transiently transfected CHO cells, cells were washed twice with ice-cold PBS and lysed 30 min on ice with RIPA buffer. After centrifugation, supernatants were cleared with protein A/G–agarose beads (Santa Cruz Biotechnology, Inc.) for 3 h at 4°C, then incubated with corresponding antibodies or control IgG for 1.5 h at 4°C followed by precipitation with protein A/G–agarose beads for 1 h at 4°C. The beads were washed three times with RIPA buffer and twice with PBS, then analyzed by immunoblotting.

Isolation of cytosolic, total membrane, and lipid raft fractions

Brain homogenates were prepared using a Potter homogenizer in HOMO buffer (1 mM $MgCl_2$, 1 mM $CaCl_2$, 1 mM $NaHCO_3$, and 5 mM Tris, pH 7.4) containing 0.32 M sucrose (HOMO-A) and centrifuged at 700 *g* for 10 min at 4°C to pellet nuclei and mitochondria. The resulted supernatants were centrifuged at 100,000 *g* at 4°C for 30 min. Supernatants obtained after centrifugation were used as fractions enriched in cytosolic proteins, whereas pellets were used as total membrane fractions. Rafts were isolated from total membrane fractions as described previously (Leshchyns'ka et al., 2003). In brief, membranes were resuspended in ice-cold TBS, pH 7.5, and extracted for 20 min on ice with 4 volumes of 1% Triton X-100 in TBS. Extracted membranes were mixed with equal volume of 80% sucrose in 0.2 M sodium carbonate, overlaid sequentially with 30% sucrose in TBS, 10% sucrose in TBS, and TBS, and centrifuged at 230,000 *g* for 17 h at 4°C. The lipid raft fraction was collected at the interface between 10 and 30% sucrose, pelleted by centrifugation at 100,000 *g* for 1 h at 4°C, and resuspended in TBS. Total protein concentration was measured using the BC kit (Interchim).

Recombinant proteins

Human Fc-tagged extracellular domain of mouse NCAM and GST-tagged intracellular domains of RPTPα were used as described previously (Chen et al., 1999; Bodrikov et al., 2005). Calmodulin-dependent protein kinase IIα (CaMKIIα) was obtained from New England Biolabs, Inc.

In vitro phosphorylation

Recombinant CaMKIIα or CaMKIIα immunopurified from rat brain (BIOMOL International, L.P.) was activated according to the manufacturer's instructions. For analysis of the phosphorylation in vitro, proteins were immunoprecipitated from CHO cells, fibroblasts, or brain homogenates as described in the Immunoprecipitation and coimmunoprecipitation section. Mock immunoprecipitation with nonspecific IgG served as a control of immunoprecipitation specificity, and beads with immunoprecipitated nonspecific IgG obtained after mock immunoprecipitation were used as control in phosphorylation reactions. Beads were then washed twice with RIPA buffer, three times with TBS, and diluted in TBS. To analyze phosphorylation of recombinant RPTPα-ID, they were coupled to glutathione beads. Glutathione beads with GST coupled instead of RPTPα-ID were used as control. Beads were washed three times with TBS and diluted in TBS. Equal volumes of control beads or beads with proteins of interest were incubated for 30 min at 30°C in CaMKIIα reaction buffer (New England Biolabs, Inc.) supplemented with 200 µM ATP in the presence of activated CaMKIIα, then washed with TBS, centrifuged for 1 min, and used for Western blot analysis or protein phosphorylation estimation.

Estimation of the serine phosphorylation of RPTPα

Serine/threonine phosphorylation was analyzed by the alkaline hydrolysis of phosphate from seryl and threonyl residues in phosphoproteins. Because mutations of Ser180 and Ser204 within RPTPα-ID completely inhibited serine/threonine phosphorylation of RPTPα, we refer to this method as to the analysis of serine phosphorylation of RPTPα throughout the text. In brief, beads containing phosphorylated and control proteins were treated with 1 N NaOH for 30 min at 65°C. The reaction was stopped by the addition of a similar volume of 3.1 N HCl, and released phosphate was measured using Malachite green phosphate detection kit (R&D Systems) according to manufacturer's instructions.

Analysis of the RPTPα phosphatase activity

Control beads and beads with immunoprecipitated RPTPα were washed twice with RIPA buffer, three times with TBS, and diluted in TBS. Glutathione beads with GST or recombinant RPTPα-ID were washed and diluted in TBS. Phosphatase activity was measured using a nonradioactive phosphatase assay system (Promega) according to manufacturer's instructions.

Gel electrophoresis and immunoblotting

Proteins were separated by 8% SDS-PAGE and electroblotted onto nitrocellulose transfer membrane (PROTRAN; Sigma-Aldrich) overnight at 5 mA. Immunoblots were blocked in milk and incubated with appropriate primary antibodies followed by incubation with peroxidase-labeled secondary antibodies and visualized using Super Signal West Pico reagents (Thermo Fisher Scientific) on BIOMAX film (Sigma-Aldrich). For immunoblots labeled with phospho-specific antibodies, 3% of BSA was used instead of milk. Molecular weight markers were prestained protein standards from Bio-Rad Laboratories. For quantitative comparisons of chemiluminescence between the lanes, the same amounts of total protein or equal amounts of immunoprecipitates were loaded in each lane. All preparations were performed three times and at least two Western blots were performed with an individual sample ($n \geq 6$). Values from all Western blots were used to calculate mean values and standard errors of the mean. The chemiluminescence quantification was performed using TINA 2.09 software (University of Manchester) or Scion Image for Windows (Scion Corporation). Group comparisons were made using a paired *t* test.

Online supplemental material

Fig. S1 shows the analysis of the Ser180 and Ser204 phosphorylation and phosphatase activity of RPTPαWT, expressed in RPTPα-negative fibroblasts alone or together with NCAM120 or NCAM180, after application of NCAM polyclonal antibodies or nonspecific rabbit IgG to transfected fibroblasts. Fig. S2 shows the analysis of the RPTPαWT phosphorylation and CaMKIIα, PKCδ, and fyn activation in CHO cells that were cotransfected with RPTPαWT and NCAM120, NCAM140, NCAM180, or GFP and treated with NCAM antibodies or nonspecific rabbit IgG. Fig. S3 shows levels of activated CaMKIIα in lipid rafts from NCAM+/+ and NCAM−/− brains, and provides the analysis of the influence of lipid raft disruption by methyl-β-cyclodextrin on CaMKIIα activation and RPTPα phosphorylation and activation in NCAM140-transfected CHO cells. Fig. S4 contains a comparison of the effects of NCAM clustering by polyclonal or monoclonal antibodies against the extracellular domain of NCAM or by NCAM-Fc on fyn activation in RPTPα-negative fibroblasts cotransfected with NCAM140 and RPTPαWT. Fig. S5 shows the time course of NCAM-dependent fyn and CaMKIIα activation in dissociated hippocampal neurons treated with NCAM monoclonal antibodies or nonspecific rat IgG. Online supplemental material is available at http://www.jcb.org/cgi/content/full/jcb.200803045/DC1.

The authors are grateful to Achim Dahlmann for genotyping, Eva Kronberg for maintenance of animals, Dr. Harold Cremer for NCAM−/− mice, Dr. Catherine J. Pallen for the plasmid encoding the intracellular domain of RPTPα, Dr. Patricia Maness for plasmid encoding NCAM140 and NCAM180, Dr. Elisabeth Bock for a plasmid encoding NCAM120, and Dr. Markus Delling for the palmitoylation deficient mutated form of NCAM140.

The authors are also grateful to the Deutsche Forschungsgemeinschaft (grant DFG SY 43/2-3 to V. Sytnyk, I. Leshchyns'ka, and M. Schachner) for support.

Submitted: 10 March 2008
Accepted: 21 August 2008

References

Beggs, H.E., P. Soriano, and P.F. Maness. 1994. NCAM-dependent neurite outgrowth is inhibited in neurons from Fyn-minus mice. *J. Cell Biol.* 127:825–833.

Beggs, H.E., S.C. Baragona, J.J. Hemperly, and P.F. Maness. 1997. NCAM140 interacts with the focal adhesion kinase p125(fak) and the SRC-related tyrosine kinase p59(fyn). *J. Biol. Chem.* 272:8310–8319.

Bhandari, V., K.L. Lim, and C.J. Pallen. 1998. Physical and functional interactions between receptor-like protein-tyrosine phosphatase alpha and p59fyn. *J. Biol. Chem.* 273:8691–8698.

Blanchetot, C., and J. den Hertog. 2000. Multiple interactions between receptor protein-tyrosine phosphatase (RPTP) alpha and membrane-distal protein-tyrosine phosphatase domains of various RPTPs. *J. Biol. Chem.* 275:12446–12452.

Bodrikov, V., I. Leshchyns'ka, V. Sytnyk, J. Overvoorde, J. den Hertog, and M. Schachner. 2005. RPTPα is essential for NCAM-mediated p59fyn activation and neurite elongation. *J. Cell Biol.* 168:127–139.

Brandt, D.T., A. Goerke, M. Heuer, M. Gimona, M. Leitges, E. Kremmer, R. Lammers, H. Haller, and H. Mischak. 2003. Protein kinase C delta induces Src kinase activity via activation of the protein tyrosine phosphatase PTP alpha. *J. Biol. Chem.* 278:34073–34078.

Buist, A., C. Blanchetot, L.G. Tertoolen, and J. den Hertog. 2000. Identification of p130cas as an in vivo substrate of receptor protein-tyrosine phosphatase alpha. *J. Biol. Chem.* 275:20754–20761.

Bukalo, O., N. Fentrop, A.Y. Lee, B. Salmen, J.W. Law, C.T. Wotjak, M. Schweizer, A. Dityatev, and M. Schachner. 2004. Conditional ablation of the neural cell adhesion molecule reduces precision of spatial learning, long-term potentiation, and depression in the CA1 subfield of mouse hippocampus. *J. Neurosci.* 24:1565–1577.

Cavallaro, U., and G. Christofori. 2004a. Multitasking in tumor progression: signaling functions of cell adhesion molecules. *Ann. N. Y. Acad. Sci.* 1014:58–66.

Cavallaro, U., and G. Christofori. 2004b. Cell adhesion and signalling by cadherins and Ig-CAMs in cancer. *Nat. Rev. Cancer.* 4:118–132.

Chen, S., N. Mantei, L. Dong, and M. Schachner. 1999. Prevention of neuronal cell death by neural adhesion molecules L1 and CHL1. *J. Neurobiol.* 38:428–439.

Cremer, H., R. Lange, A. Christoph, M. Plomann, G. Vopper, J. Roes, R. Brown, S. Baldwin, P. Kraemer, S. Scheff, et al. 1994. Inactivation of the N-CAM gene in mice results in size reduction of the olfactory bulb and deficits in spatial learning. *Nature.* 367:455–459.

den Hertog, J., and T. Hunter. 1996. Tight association of GRB2 with receptor protein-tyrosine phosphatase alpha is mediated by the SH2 and C-terminal SH3 domains. *EMBO J.* 15:3016–3027.

den Hertog, J., S. Tracy, and T. Hunter. 1994. Phosphorylation of receptor protein-tyrosine phosphatase alpha on Tyr789, a binding site for the SH3-SH2-SH3 adaptor protein GRB-2 in vivo. *EMBO J.* 13:3020–3032.

den Hertog, J., J. Sap, C.E. Pals, J. Schlessinger, and W. Kruijer. 1995. Stimulation of receptor protein-tyrosine phosphatase alpha activity and phosphorylation by phorbol ester. *Cell Growth Differ.* 6:303–307.

Gennarini, G., M. Hirn, H. Deagostini-Bazin, and C. Goridis. 1984. Studies on the transmembrane disposition of the neural cell adhesion molecule N-CAM. The use of liposome-inserted radioiodinated N-CAM to study its transbilayer orientation. *Eur. J. Biochem.* 142:65–73.

Helmke, S., K. Lohse, K. Mikule, M.R. Wood, and K.H. Pfenninger. 1998. SRC binding to the cytoskeleton, triggered by growth cone attachment to laminin, is protein tyrosine phosphatase-dependent. *J. Cell Sci.* 111:2465–2475.

Hudmon, A., E. Lebel, H. Roy, A. Sik, H. Schulman, M.N. Waxham, and P. De Koninck. 2005. A mechanism for Ca2+/calmodulin-dependent protein kinase II clustering at synaptic and nonsynaptic sites based on self-association. *J. Neurosci.* 25:6971–6983.

Jessen, U., V. Novitskaya, N. Pedersen, P. Serup, V. Berezin, and E. Bock. 2001. The transcription factors CREB and c-Fos play key roles in NCAM-mediated neuritogenesis in PC12-E2 cells. *J. Neurochem.* 79:1149–1160.

Kiryushko, D., I. Korshunova, V. Berezin, and E. Bock. 2006. Neural cell adhesion molecule induces intracellular signaling via multiple mechanisms of Ca2+ homeostasis. *Mol. Biol. Cell.* 17:2278–2286.

Kiselyov, V.V., V. Soroka, V. Berezin, and E. Bock. 2005. Structural biology of NCAM homophilic binding and activation of FGFR. *J. Neurochem.* 94:1169–1179.

Kolkova, K., H. Stensman, V. Berezin, E. Bock, and C. Larsson. 2005. Distinct roles of PKC isoforms in NCAM-mediated neurite outgrowth. *J. Neurochem.* 92:886–894.

Korshunova, I., V. Novitskaya, D. Kiryushko, N. Pedersen, K. Kolkova, E. Kropotova, M. Mosevitsky, M. Rayko, J.S. Morrow, I. Ginzburg, et al. 2007. GAP-43 regulates NCAM-180-mediated neurite outgrowth. *J. Neurochem.* 100:1599–1612.

Leshchyns'ka, I., V. Sytnyk, J.S. Morrow, and M. Schachner. 2003. Neural cell adhesion molecule (NCAM) association with PKCβ2 via βI spectrin is implicated in NCAM-mediated neurite outgrowth. *J. Cell Biol.* 161:625–639.

Leshchyns'ka, I., V. Sytnyk, M. Richter, A. Andreyeva, D. Puchkov, and M. Schachner. 2006. The adhesion molecule CHL1 regulates uncoating of clathrin-coated synaptic vesicles. *Neuron.* 52:1011–1025.

Liang, L., K.L. Lim, K.T. Seow, C.H. Ng, and C.J. Pallen. 2000. Calmodulin binds to and inhibits the activity of the membrane distal catalytic domain of receptor protein-tyrosine phosphatase alpha. *J. Biol. Chem.* 275:30075–30081.

Lüthi, A., J.P. Laurent, A. Figurov, D. Muller, and M. Schachner. 1994. Hippocampal long-term potentiation and neural cell adhesion molecules L1 and NCAM. *Nature.* 372:777–779.

Maness, P.F., and M. Schachner. 2007. Neural recognition molecules of the immunoglobulin superfamily: signalling transducers of axon guidance and neuronal migration. *Nat. Neurosci.* 10:19–26.

Niethammer, P., M. Delling, V. Sytnyk, A. Dityatev, K. Fukami, and M. Schachner. 2002. Cosignaling of NCAM via lipid rafts and the FGF receptor is required for neuritogenesis. *J. Cell Biol.* 157:521–532.

Ohbayashi, K., H. Fukura, H.K. Inoue, Y. Komiya, and M. Igarashi. 1998. Stimulation of L-type Ca2+ channel in growth cones activates two independent signaling pathways. *J. Neurosci. Res.* 51:682–696.

Paratcha, G., F. Ledda, and C.F. Ibanez. 2003. The neural cell adhesion molecule NCAM is an alternative signaling receptor for GDNF family ligands. *Cell.* 113:867–879.

Pollerberg, G.E., M. Schachner, and J. Davoust. 1986. Differentiation state-dependent surface mobilities of two forms of the neural cell adhesion molecule. *Nature.* 324:462–465.

Pollerberg, G.E., K. Burridge, K.E. Krebs, S.R. Goodman, and M. Schachner. 1987. The 180-kD component of the neural cell adhesion molecule N-CAM is involved in a cell-cell contacts and cytoskeleton-membrane interactions. *Cell Tissue Res.* 250:227–236.

Rutishauser, U., A. Acheson, A.K. Hall, D.M. Mann, and J. Sunshine. 1988. The neural cell adhesion molecule (NCAM) as a regulator of cell-cell interactions. *Science.* 240:53–57.

Santuccione, A., V. Sytnyk, I. Leshchyns'ka, and M. Schachner. 2005. Prion protein recruits its neuronal receptor NCAM to lipid rafts to activate p59fyn and to enhance neurite outgrowth. *J. Cell Biol.* 169:341–354.

Schmid, R.S., R.D. Graff, M.D. Schaller, S. Chen, M. Schachner, J.J. Hemperly, and P.F. Maness. 1999. NCAM stimulates the Ras-MAPK pathway and CREB phosphorylation in neuronal cells. *J. Neurobiol.* 38:542–558.

Schuch, U., M.J. Lohse, and M. Schachner. 1989. Neural cell adhesion molecules influence second messenger systems. *Neuron.* 3:13–20.

Stetak, A., P. Csermely, A. Ullrich, and G. Keri. 2001. Physical and functional interactions between protein tyrosine phosphatase alpha, PI 3-kinase, and PKCdelta. *Biochem. Biophys. Res. Commun.* 288:564–572.

Sytnyk, V., I. Leshchyns'ka, M. Delling, G. Dityateva, A. Dityatev, and M. Schachner. 2002. Neural cell adhesion molecule promotes accumulation of TGN organelles at sites of neuron-to-neuron contacts. *J. Cell Biol.* 159:649–661.

Sytnyk, V., I. Leshchyns'ka, A.G. Nikonenko, and M. Schachner. 2006. NCAM promotes assembly and activity-dependent remodeling of the postsynaptic signaling complex. *J. Cell Biol.* 174:1071–1085.

Tracy, S., P. van der Geer, and T. Hunter. 1995. The receptor-like protein-tyrosine phosphatase, RPTP alpha, is phosphorylated by protein kinase C on two serines close to the inner face of the plasma membrane. *J. Biol. Chem.* 270:10587–10594.

Walmod, P.S., K. Kolkova, V. Berezin, and E. Bock. 2004. Zippers make signals: NCAM-mediated molecular interactions and signal transduction. *Neurochem. Res.* 29:2015–2035.

Williams, E.J., F.S. Walsh, and P. Doherty. 1994. The production of arachidonic acid can account for calcium channel activation in the second messenger pathway underlying neurite outgrowth stimulated by NCAM, N-cadherin, and L1. *J. Neurochem.* 62:1231–1234.

Williams, E.J., B. Mittal, F.S. Walsh, and P. Doherty. 1995. A Ca2+/calmodulin kinase inhibitor, KN-62, inhibits neurite outgrowth stimulated by CAMs and FGF. *Mol. Cell. Neurosci.* 6:69–79.

Zheng, X.M., Y. Wang, and C.J. Pallen. 1992. Cell transformation and activation of pp60c-src by overexpression of a protein tyrosine phosphatase. *Nature.* 359:336–339.

Zheng, X.M., R.J. Resnick, and D. Shalloway. 2000. A phosphotyrosine displacement mechanism for activation of Src by PTPalpha. *EMBO J.* 19:964–978.

Zheng, X.M., R.J. Resnick, and D. Shalloway. 2002. Mitotic activation of protein-tyrosine phosphatase alpha and regulation of its Src-mediated transforming activity by its sites of protein kinase C phosphorylation. *J. Biol. Chem.* 277:21922–21929.